Helsinki University of Technology
Low Temperature Laboratory
Espoo 2004

JOSEPHSON EFFECTS AND TEXTURAL DYNAMICS IN SUPERFLUID HELIUM THREE

Janne Viljas

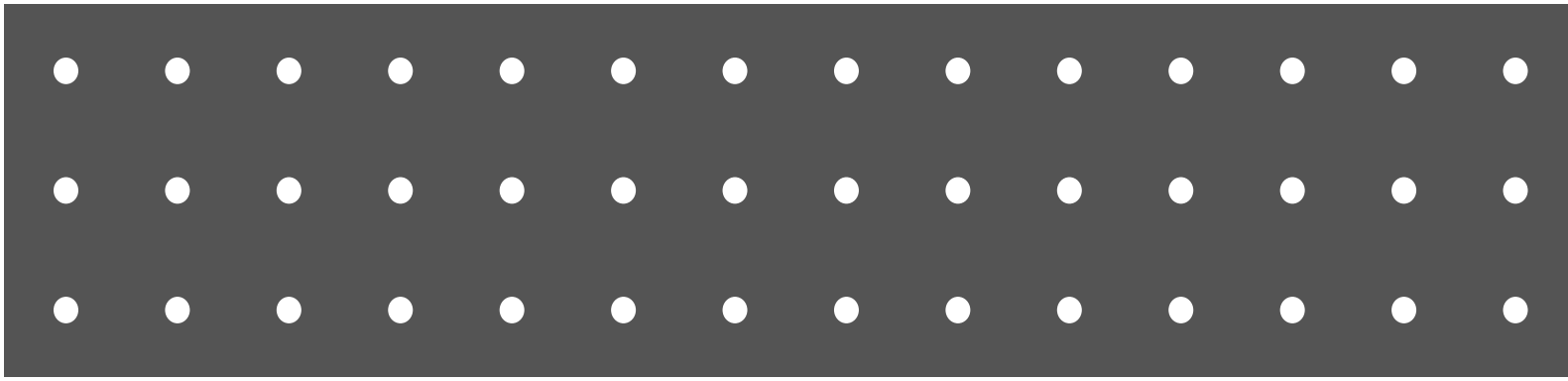

TEKNILLINEN KORKEAKOULU
TEKNISKA HÖGSKOLAN
HELSINKI UNIVERSITY OF TECHNOLOGY
TECHNISCHE UNIVERSITÄT HELSINKI
UNIVERSITE DE TECHNOLOGIE D'HELSINKI

JOSEPHSON EFFECTS AND TEXTURAL DYNAMICS IN SUPERFLUID HELIUM THREE

Janne Viljas

Dissertation for the degree of Doctor of Science in Technology to be presented with due permission of the Department of Engineering Physics and Mathematics for public examination and debate in Auditorium F1 at Helsinki University of Technology (Espoo, Finland) on the 4th of June, 2004, at 12 o'clock noon.

Helsinki University of Technology
Department of Engineering Physics and Mathematics
Low Temperature Laboratory

Teknillinen korkeakoulu
Teknillisen fysiikan ja matematiikan osasto
Kylmälaboratorio

Distribution:
Helsinki University of Technology
Low Temperature Laboratory
P.O. Box 2200
FIN-02015 HUT
Tel. +358-9-451-2968
Fax. +358-9-451-2969
E-mail: Janne.Viljas@hut.fi
This dissertation can be read at http://lib.hut.fi/Diss/

ISBN 951-22-7008-0
ISBN 951-22-7009-9 (pdf)

Otamedia Oy
Espoo 2004

HELSINKI UNIVERSITY OF TECHNOLOGY
P.O. BOX 1000, FIN-02015 HUT
http://www.hut.fi

ABSTRACT OF DOCTORAL DISSERTATION

Author Janne Kalevi Viljas

Name of the dissertation

JOSEPHSON EFFECTS AND TEXTURAL DYNAMICS IN SUPERFLUID HELIUM THREE

Date of manuscript 24.2.2004 | Date of the dissertation 4.6.2004

☐ Monograph ☑ Article dissertation (summary + original articles)

Department Department of Engineering Physics and Mathematics
Laboratory Low Temperature Laboratory
Field of research Theoretical low-temperature physics
Opponent(s) Prof. James A. Sauls
Supervisor Prof. Martti M. Salomaa
(Instructor) Prof. Erkki V. Thuneberg

Abstract

As liquid helium three is cooled to temperatures below 1 mK, it becomes a superfluid. In this state it is able to support dissipationless mass supercurrents. Analogously to what happens for superconducting metals, when two volumes of the superfluid are brought into contact through a "weak link", phenomena known as Josephson effects arise. These are associated with supercurrents which depend periodically on the difference between the quantum-mechanical phases of the superfluid order parameters. However, the order parameter in helium three is far more complicated than that in conventional superconductors, and this gives rise to new features in the physics of weak links.

In this thesis we present theoretical and numerical considerations of the Josephson effects and dissipative currents in weak links of superfluid helium three, in particular its B phase. We use our results to analyze recent experiments.

In the case of small point contacts, we calculate the equilibrium current-phase relations, as well as the dissipative currents due to multiple Andreev reflections when the contact is biased by a pressure head. These calculations are made using quasiclassical theory. We take self-consistently into account the effects of microscopically rough surfaces on the order parameter, which is important for obtaining quantitatively correct results. For apertures whose sizes are on the order of the temperature-dependent coherence length, we compute current-phase relations using Ginzburg-Landau theory. In this case we also consider weak links involving the superfluid A phase. Using a hydrodynamical approach to the B phase, we also consider large arrays of apertures, where we introduce the new concept of "anisotextural" Josephson effect. This effect depends crucially on the presence of the spin-orbit degrees of freedom in the order parameter, and is not possible in conventional superconductors. We use this concept to interpret experiments made with array-type weak links, where so-called "pi-states" and unexpected dissipation effects were found.

Keywords superfluidity, Josephson effect, helium-3, texture, quasiclassical theory

UDC | Number of pages 35

ISBN (printed) 951-22-7008-0 | ISBN (pdf) 951-22-7009-9

ISBN (others) | ISSN

Publisher Helsinki University of Technology, Low Temperature Laboratory

Print distribution

☑ The dissertation can be read at http://lib.hut.fi/Diss/

Acknowledgments

During the years of making this thesis at the Low Temperature Laboratory (LTL), I have benefited from help and advice from a number of people. Prof. Mikko Paalanen, the director of LTL, and Prof. Matti Krusius are thanked for making this possible, and for providing an interesting environment for research work. The office staff Pirjo Kinanen, Liisi Pasanen, Teija Halme, Satu Pakarinen, Tuire Koivisto, and Marja Holmström are gratefully acknowledged for keeping things running smoothly.

The biggest expression of gratitude I owe to my instructor, Prof. Erkki Thuneberg, who taught me most of what I know about physics research. My pre-examiners S.-K. Yip and M. Fogelström are acknowledged for checking the thesis and for providing useful remarks. My supervisor Prof. Martti Salomaa is also thanked for his comments on the manuscript.

Big thanks are also due to my long-term roommates Risto Hänninen and Juha Kopu, for support and helpful discussions. In addition I want to thank A. Finne, M. Sillanpää, R. Lindell, L. Roschier, T. Heikkilä, T. Ruokola, J. Ruohio, R. Blaauwgeers, A. Schakel, M. Nishida, N. Hatakenaka, G. Volovik, N. Kopnin, P. Hakonen, R. Simmonds, O. Avenel, E. Varoquaux, Yu. Mukharsky, S. Pereverzev, G. Eska, D. Rainer, J. Sauls, and all others I have had some useful contact with, as far as work is considered.

I also thank my friends and acquaintances with whom I have shared some of my spare time during the past few years. And I thank my parents and my sister, and all of our family for supporting me in my studies of this rather specialized field of human endeavor.

Finally, I wish to honor the late academician Olli Lounasmaa, the creator of LTL. I did not have much personal contact with him, but our last encounter, which took place by the lab's coffee machine shortly before his passing away in late 2002, may be worth recording for posterity. Apparently on that day Olli was worried about the ever-increasing number of "product placements" in mainstream cinematography. Or so I gathered when he suddenly asked me what I thought about James Bond's new habit of using Finlandia vodka in his well-known favorite drink. I answered, without hesitation, that I was happy to see Bond drinking Finlandia rather than a certain other brand. After that I never saw Olli again.

Otaniemi, April 2004

Janne Viljas

List of Publications

[P1] J. K. Viljas and E. V. Thuneberg, *Theory of the π state in ^{3}He Josephson junctions*, Phys. Rev. Lett. **83**, 3868-3871 (1999). ©1999 American Physical Society.

[P2] J. K. Viljas and E. V. Thuneberg, *Pinhole calculations of the Josephson effect in ^{3}He-B*, Phys. Rev. B **65**, 064530:1-19 (2002). ©2002 American Physical Society.

[P3] J. K. Viljas and E. V. Thuneberg, *Equilibrium simulations of 2D weak links in p-wave superfluids*, J. Low Temp. Phys **129**, 423-471 (2002). ©2002 Plenum Publishing Corporation.

[P4] J. K. Viljas and E. V. Thuneberg, *Stability of A-B phase boundary in a constriction*, Physica B **329-333**, 86-87 (2003). ©2003 Elsevier Science.

[P5] J. K. Viljas and E. V. Thuneberg, *Dissipative currents in superfluid ^{3}He-B weak links*, J. Low Temp. Phys. **134**, 743-748 (2004). ©2004 Plenum Publishing Corporation.

[P6] J. K. Viljas and E. V. Thuneberg, *Dissipative currents in superfluid ^{3}He Weak Links*, Report TKK-KYL-011 (2004), submitted to Phys. Rev. Lett.

Author's contribution

The research for this thesis has been done in close collaboration with my instructor, Prof. Erkki Thuneberg. His contributions to formulating the problems, and to the analytical work (in particular, the energy functional in [P2]), was most prominent in the earliest papers [P1] and [P2]. However, generally all of the numerical work, and also most of the analytical work related to publications [P3-P6], was carried out by me. In these latter publications I have also formulated the majority of the problems by myself. I have participated in the preparation of the articles at all stages. In publication [P1] I am mostly responsible for generating the figures. The first drafts and large parts of the published version of [P2] were written by me. Publications [P3-P5] were mostly written by me, and so was the first version of [P6].

Contents

1 Introduction

This thesis consists of theoretical and numerical studies of the so-called Josephson effects in weak links of superfluid ^{3}He. The name for these phenomena derives from B. D. Josephson, who first predicted their existence in tunneling junctions between two superconductors in 1962 [1]. Since their experimental discovery shortly thereafter, the superconductor Josephson effects have been extensively studied, and important applications for them exist [2, 3]. By analogy, similar phenomena should also exist in the low-temperature superfluid phases of liquid helium [4], as well as in Bose-Einstein condensed dilute atomic gases [5]. In superfluid ^{3}He they were first observed in the late 1980's in experiments by Avenel and Varoquaux in Paris [6–8], whereas in superfluid ^{4}He evidence of pure Josephson-like behavior was not seen until very recently [9]. Around the initial experimental discovery of the effects in ^{3}He, a burst of theoretical calculations already appeared [10–18]. The calculations in this thesis, however, are mostly related to the interpretation of newer experiments made at Berkeley [19–22] and in Paris [23] which revealed some unexpected phenomena. These are the so-called "π states", and certain features of the dissipative currents observed in the Berkeley experiments. Effects rather similar to the π states are known to exist in superconducting weak links between unconventional superconductors [24–26], and in the presence of spin-active interfaces [27], for example. These are also related to what are known as "π junctions" [28]. Soon after the Berkeley experiments, analogous theoretical ideas were applied to the case of ^{3}He as well [29]. In addition to generalizing the calculations of Ref. [29] somewhat, we have analyzed the Berkeley data on the π states and the dissipation phenomena by using a more ^{3}He-specific concept which we call an "anisotextural" effect. This is the central concept of this thesis. Other theoretical work related to the same experiments have been presented in Refs. [30–34].

In contrast to their superconductor cousins, no practical applications for the superfluid Josephson effects exist, although some progress has been made in using them in superfluid gyroscopes [35, 36]. Nevertheless, in view of basic science, the case of superfluid ^{3}He provides a very interesting topic for research, as also this thesis aims to demonstrate.

1.1 Superfluid ^{3}He

The atoms in liquid ^{3}He are neutral spin-1/2 fermions. At temperatures T much lower than the Fermi temperature T_F this many-body system becomes a strongly degenerate quantum liquid with a well-defined Fermi surface. This is known as a *Fermi liquid* [37]. At normal pressures the liquid never solidifies.

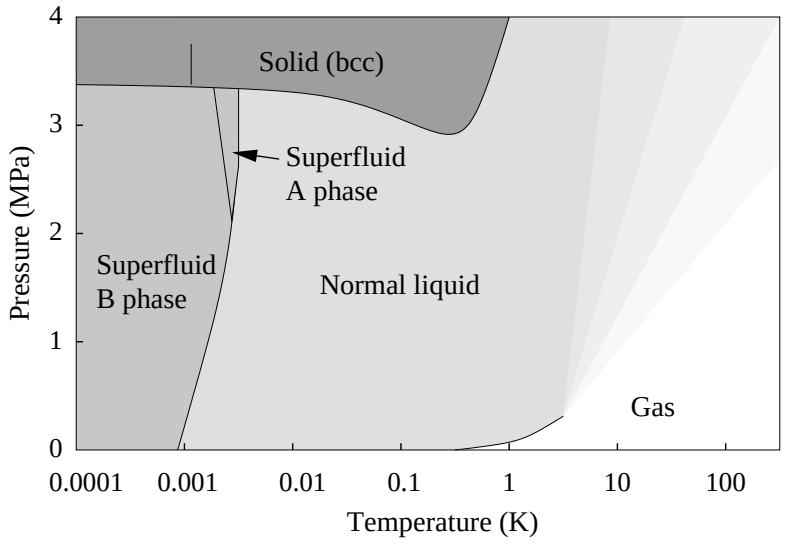

Figure 1: Phase diagram of ^{3}He in zero external magnetic field.

Instead, below a critical temperature $T_c \approx 1$ mK the Fermi surface becomes unstable, and the system undergoes a phase transition into a superfluid state where the atoms form Cooper pairs, much like the conduction electrons in superconducting metals do [38]. However, whereas in conventional superconductors the pairs have spin $S = 0$ and relative angular momentum $L = 0$ (singlet s wave) [3], in ^{3}He they have $S = 1$ and $L = 1$ (triplet p wave). The pairing state is described by the gap matrix

$$\underline{\Delta}(\hat{\mathbf{k}}) = \mathbf{\Delta}(\hat{\mathbf{k}}) \cdot \underline{\boldsymbol{\sigma}} \mathrm{i} \underline{\sigma}_y = \begin{bmatrix} -\Delta_x + \mathrm{i}\Delta_y & \Delta_z \\ \Delta_z & \Delta_x + \mathrm{i}\Delta_y \end{bmatrix}, \tag{1}$$

where $\underline{\sigma}_\alpha$ with $\alpha = x, y, z$ are the Pauli matrices, $\mathbf{\Delta}(\hat{\mathbf{k}})$ is a complex-valued spin vector, and $\hat{\mathbf{k}}$ parametrizes its angular dependence of positions on the spherical Fermi surface [38]. The quantity $|\mathbf{\Delta}(\hat{\mathbf{k}})|$ is called an energy gap, and it is the minimum energy per particle needed for creating a *quasiparticle excitation* at the position $\hat{\mathbf{k}}$. Since the angular part should correspond to $L = 1$ pairs, $\mathbf{\Delta}(\hat{\mathbf{k}})$ may be represented in the form

$$\Delta_\mu(\hat{\mathbf{k}}) = \sum_{i=x,y,z} A_{\mu i} \hat{k}_i, \quad \mu = x, y, z. \tag{2}$$

The matrix formed by the nine complex coefficients $A_{\mu i}$ is usually referred to as the *order parameter* of the superfluid state.

In the absence of external magnetic fields, there are two stable bulk phases in which the superfluid can exist: the A phase and the B phase, see Fig. 1. The A phase corresponds to

$$A_{\mu i} = \Delta_A \hat{d}_\mu (\hat{m}_i + \mathrm{i}\hat{n}_i) \quad \text{(A phase)}, \tag{3}$$

where $\hat{\mathbf{d}}, \hat{\mathbf{m}}, \hat{\mathbf{n}}$ are unit vectors, with $\hat{\mathbf{m}} \perp \hat{\mathbf{n}}$. The vector $\hat{\mathbf{l}} = \hat{\mathbf{m}} \times \hat{\mathbf{n}}$ describes the direction of the angular momentum of the pairs, while $\hat{\mathbf{d}}$ is in a direction along which their spin vanishes. In this case $\underline{\Delta}$ may be diagonalized such that the condensate only consists of equal amounts of $S_z = \pm 1$ ($\uparrow\uparrow$ and $\downarrow\downarrow$) pairs. The energy gap $|\mathbf{\Delta}(\hat{\mathbf{k}})|$ is anisotropic, vanishing for $\hat{\mathbf{k}} \parallel \hat{\mathbf{l}}$. The B phase, on the other hand, has

$$A_{\mu i} = \Delta_B e^{\mathrm{i}\varphi} R_{\mu i}(\hat{\mathbf{n}}, \theta) \quad \text{(B phase)}. \tag{4}$$

Here $R(\hat{\mathbf{n}}, \theta)$ is a rotation matrix between the spin and orbital degrees of freedom, where $\hat{\mathbf{n}}$ and θ are its rotation axis and angle, respectively. The B phase contains all $S_z = 0, \pm 1$ ($\uparrow\downarrow + \downarrow\uparrow$, $\uparrow\uparrow$, and $\downarrow\downarrow$) pairs in equal amounts, and has an isotropic gap $|\mathbf{\Delta}(\hat{\mathbf{k}})| = \Delta_B \equiv \Delta$. In this thesis I mostly concentrate on this phase, whose stability region covers most of the phase diagram in the superfluid state at zero external magnetic field. Calculations involving the A phase are reported only in publications [P3] and [P4].

Equations (3) and (4) are only valid in the unperturbed bulk liquid. Close to solid surfaces collision processes lead to breaking of Cooper pairs and thus to a suppression of the order parameter [39, 40]. Close to a planar wall the B-phase order parameter is more generally of the form [P2]

$$\mathbf{\Delta}(\hat{\mathbf{k}}, z) = e^{\mathrm{i}\varphi} R(\hat{\mathbf{n}}, \theta)[\Delta_\parallel(z)\hat{k}_x, \Delta_\parallel(z)\hat{k}_y, \Delta_\perp(z)\hat{k}_z]^T, \tag{5}$$

where the z axis is chosen perpendicular to the wall. The components $\Delta_\parallel$ and $\Delta_\perp$ are shown in Fig. 2 for smooth (specular) and microscopically rough (diffusive) surfaces. Often the gap-suppressing effect of the wall is neglected to simplify calculations, but we have taken it self-consistently into account in all of our numerical work.

1.2 Hydrostatic theory of the B phase

Physically, the superfluid state is manifested in the existence of supercurrents, *i.e.*, currents which can flow without viscosity. For example, a persistent current may be established around a toroidal container, which does not decay provided that the temperature T is kept below T_c. Since the ^{3}He atoms are neutral, the properties of superfluid ^{3}He are in some respects similar to

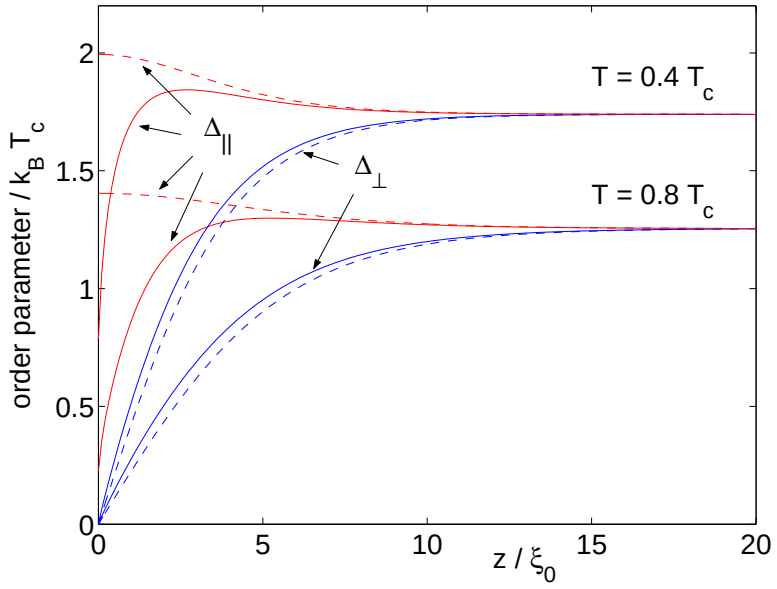

Figure 2: Components $\Delta_{\|}$ and $\Delta_{\perp}$ of the order parameter for a diffusive wall (solid lines) and for a specular wall (dashed lines) at two temperatures. Here z is the distance from the wall, and ξ_0 is the zero-temperature coherence length (see below).

an extreme type-II superconductor where the magnetic screening length is infinite [3]. In particular, the supercurrents can flow everywhere in the bulk liquid and are not restricted to the boundaries of the sample. A simple, phenomenological way to describe the superfluid is the so-called two-fluid model [37]. In this model the fluid, with total mass density ρ, is divided into two interpenetrating components which have their own separate dynamics. These are the *superfluid* (with density ρ_s and velocity $\mathbf{v}_s$) which corresponds to the Cooper-paired condensate, and the *normal fluid* (with density ρ_n and velocity $\mathbf{v}_n$) consisting of thermal quasiparticle excitations. The total mass densities satisfy $\rho = \rho_s + \rho_n$, and the current density is given by $\mathbf{j} = \mathbf{j}_s + \mathbf{j}_n = \rho_s \mathbf{v}_s + \rho_n \mathbf{v}_n$. For the B phase, ρ_s is isotropic.

In equilibrium, the normal fluid is at rest, and it is often sufficient to consider the superfluid part alone. The superfluid velocity $\mathbf{v}_s$ is given by the gradient of the complex phase φ of the order parameter, such that

$$\begin{aligned} \mathbf{j}_s &= \rho_s \mathbf{v}_s \\ \mathbf{v}_s &= (\hbar/2m_3)\boldsymbol{\nabla}\varphi, \end{aligned} \tag{6}$$

where $\hbar$ is Planck's constant h divided by 2π and m_3 is the mass of a ^{3}He atom

[38]. Due to triplet pairing, there can also exist so-called spin supercurrents [41]. These are currents where the "↑↑ and ↓↓" parts of the condensate flow in opposite directions, creating a magnetization current in the absence of net mass transport. Analogously to Eqs. (6), the spin current $\mathbf{j}_\alpha^{sp}$ and spin velocity $\mathbf{v}_\alpha^{sp}$ for spin projections $\alpha = x, y, z$ are obtained from

$$\begin{aligned} j_{\alpha i}^{sp} &= \rho_{\alpha\beta,ij}^{sp} v_{\beta j}^{sp} \\ \mathbf{v}_\alpha^{sp} &= -(\hbar/4m_3)\epsilon_{\alpha\beta\gamma} R_{\beta j} \boldsymbol{\nabla} R_{\gamma j}, \end{aligned} \tag{7}$$

where (as always below) summation over repeated indices is implied. The "spin superfluid density" is of the form $\rho_{\alpha\beta,ij}^{sp} = [\rho_1^{sp}\delta_{\alpha\beta}\delta_{ij} + \rho_2^{sp} R_{\alpha i} R_{\beta j} + \rho_3^{sp} R_{\alpha j} R_{\beta i}]$ [42]. To leading order in the gradients, the kinetic energy of the fluid (assuming $\mathbf{v}_n = \mathbf{0}$) may be written as

$$F_G = \frac{1}{2}\int \mathrm{d}^3 r [\rho_s \mathbf{v}_s^2 + \rho_{\alpha\beta,ij}^{sp} v_{\alpha i}^{sp} v_{\beta j}^{sp}]. \tag{8}$$

One important thing to note here is that, in this order of approximation, the mass and spin currents are *decoupled*.

This type of large-scale description of the superfluid in terms of the "soft degrees of freedom" φ and R, assuming the amplitude of $\underline{\Delta}$ to be constant, belongs to the field of *hydrodynamic theory* [38]. In publications [P1] and [P2], we only consider it in the stationary limit where it reduces to the much simpler theory of *hydrostatics* [43]. Regions where $\underline{\Delta}$ is locally suppressed or where its bulk form is modified enter the hydrostatic theory only through boundary conditions or phenomenological interaction terms for R. These involve many coupling constants whose values may be calculated from lower-level theories such as the *quasiclassical theory* [42]. In publication [P2], we have used this method to calculate some of the surface-interaction parameters. Two of them are b_2 and b_4 in the surface-dipole energy

$$F_{SD} = \int \mathrm{d}^2 r [b_4(\hat{\mathbf{n}}\cdot\hat{\mathbf{s}})^4 - b_2(\hat{\mathbf{n}}\cdot\hat{\mathbf{s}})^2], \tag{9}$$

where $\hat{\mathbf{s}}$ is the surface normal. They are obtained as by-products of computing the order parameters of Fig. 2 [43]. Previously they have been known in the Ginzburg-Landau (GL) regime only, *i.e.*, for T close to T_c. We also note the form of the bulk dipole-dipole interaction

$$F_D = 8 g_D \Delta^2 \int \mathrm{d}^3 r \left(\frac{1}{4} + \cos\theta\right)^2. \tag{10}$$

The minimum of this energy corresponds to $\theta = \theta_L \equiv \arccos(-1/4) \approx 104°$, which is the so-called "Leggett angle" [41]. We always assume $\theta = \theta_L$, unless

otherwise stated. In this case the spin part of the theory reduces to an analysis of the vector field $\hat{\mathbf{n}}$. Since different walls, for example, may favor different orientations of $\hat{\mathbf{n}}$, the vector field generally forms complicated *textures* in the experimental cell. In the absence of external magnetic fields F_{SD} is usually the only important surface interaction, and the texture is determined by a competition between its minimum (where $\hat{\mathbf{n}} \parallel \hat{\mathbf{s}}$ on all surfaces) and that of F_G (where $\hat{\mathbf{n}}$ is uniform). Similar textural phenomena are found in the physics of liquid crystals.

1.3 Basic concepts of superfluid weak links

When the superfluid is forced into small restricted geometries with dimensions approaching the temperature-dependent coherence length $\xi_{GL}(T)$, hydrodynamic theory begins to fail. A *superfluid weak link* is a constriction in a wall between two volumes of superfluid, which is so small that the order parameter is partially suppressed inside it. Thus at least one of the dimensions of the constriction (in the plane of the wall) must be on the order of $\xi_{GL} = \hbar v_F/(\sqrt{10}\Delta) \sim (1 - T/T_c)^{-1/2}$, or the zero-temperature coherence length $\xi_0 = \hbar v_F/(2\pi k_B T_c) \sim 15 \ldots 80$ nm when $T \ll T_c$. Here v_F is the Fermi velocity and k_B is Boltzmann's constant. If such a weak link is biased by a difference $\phi = \varphi^r - \varphi^l$ of the order parameter phases $\varphi^{l,r}$ on the left (l) and right (r) sides, then most of the phase drop occurs within the short distance inside the constriction. It is not possible to maintain an arbitrarily large phase difference ϕ, since in small constrictions *phase slips* occur easily. A phase slip is a process where the order parameter tends locally to zero, at which point its complex phase is undetermined and thus the system may "unwind" a multiple of 2π from ϕ. In larger flow channels this happens via the motion of quantized vortices across the flow. The maximum supercurrent which may be driven through the weak link before such dissipative phase slips occur is referred to as the *critical current*. The term *Josephson junction* is usually reserved for superconductor weak links with tunneling barriers [2], but is often used in the context of ^{3}He as a synonym for weak link.

The coupling through the weak link leads to a change in the free energy of the system. For the B phase in zero magnetic field this coupling energy may be written in the form [P1, P2, P3]

$$F_J = F_J(\phi, \psi_{ij}), \quad \psi_{ij} = R^l_{\mu i} R^r_{\mu j}, \quad i, j = x, y, z. \tag{11}$$

As for conventional superconductors, F_J depends on the phase difference ϕ [3]. However, in ^{3}He it also depends on the spin-orbit rotation matrices $R^{l,r}$ in a way which is invariant with respect to global spin rotations. Thus, unlike

in hydrostatic theory, the weak link leads to a nonlinear *coupling* between the phase and spin-orbit degrees of freedom, and hence between the mass and spin Josephson currents through the weak link. The mass supercurrent is given by

$$J_s = \frac{2m_3}{\hbar}\frac{\partial F_J}{\partial \phi} \tag{12}$$

and the spin supercurrent by [P2, P3]

$$J_\alpha^{sp} = \epsilon_{\alpha\beta\gamma} R^l_{\beta i} R^r_{\gamma j} \frac{\partial F_J}{\partial (R^l_{\mu i} R^r_{\mu j})}, \quad \alpha = x, y, z. \tag{13}$$

The ϕ-dependences $F_J(\phi)$ and $J_s(\phi)$ are generally referred to as the energy-phase relation (EPR) and the current-phase relation (CPR). They are 2π-periodic in ϕ and single-valued for small enough weak links. Publications [P1], [P2], [P3] and [P4] concentrate on studying these functions in *equilibrium*. A *nonequilibrium* situation is obtained if the weak link is biased by a pressure head P. This results in a relative shift between the chemical potentials $\mu^{l,r}$ given by $U = \mu^l - \mu^r = (m_3/\rho)P$. (The two sides are assumed to be in good thermal contact. A temperature difference would give rise to additional phenomena [44].) Consequently, ϕ evolves in time according to the ac Josephson relation [3]

$$\frac{\mathrm{d}\phi}{\mathrm{d}t} = +\frac{2U}{\hbar}. \tag{14}$$

Thus for a constant bias $\phi(t) = \omega_J t$, where $\omega_J = 2m_3 P/(\rho\hbar)$ is the Josephson frequency. Therefore the supercurrents J_s and J_α^{sp} *oscillate* periodically, with the period $T_J = 2\pi/\omega_J$. However, in general also energy-dissipating dc currents are generated, which have a finite average over T_J. The associated current-pressure ($I - P$) characteristics provide another useful way of characterizing weak links. Below we describe two mechanisms for such currents. One is the process of *multiple Andreev reflections* (MAR) and the other is due to what we call an *anisotextural* Josephson effect [P2]. The latter follows from the coupling of ϕ and ψ_{ij} in geometries where the texture is not fixed. The dissipative currents are the subject of papers [P5] and [P6].

1.4 Experiments with superfluid weak links

Experimental studies of Josephson effects in superfluids are usually based on some variants of a "membrane-aperture oscillator" [45]. Mainly two kinds of cell topologies have been used, as illustrated in Fig. 3. In both cases the

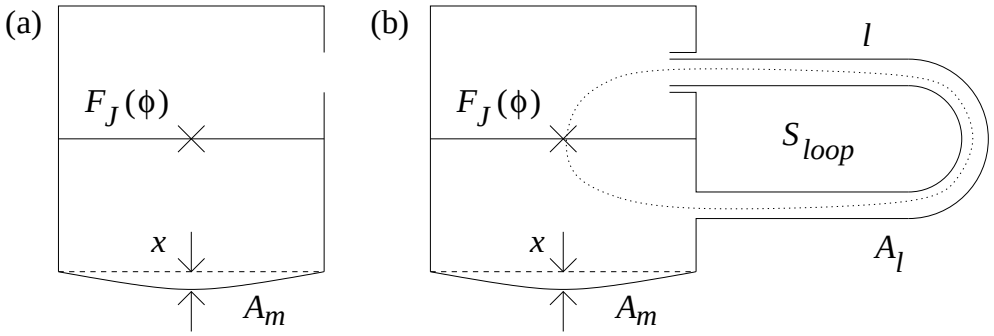

Figure 3: Schematic representation of two types of "membrane-aperture oscillator". In configuration (a) the two volumes of superfluid are only connected via the weak link (×). In configuration (b) there is an additional flow path in parallel with the weak link. The symbols are explained in the text.

cell consists of two volumes of superfluid connected by a weak link, where at least one of the volumes has a flexible membrane which may be used to drive and/or measure mass currents flowing through the weak link. The simply-connected configuration (a), where two volumes of superfluid are connected through the weak link but not otherwise, was already used in the earliest attempts to find the Josephson phenomena [46]. It was also used in the experiments done at Berkeley with whose interpretation this thesis is mostly involved [20]. The doubly-connected configuration (b) was used in the experiments of Refs. [6–9, 23, 35, 36].

In configuration (a) the current-phase relation $J_s(\phi)$ has been determined as follows [45]. Let ρ be the density of the liquid and P the relative overpressure on the membrane side. Assuming the compressibility of the fluid to be negligible, a displacement $x(t)$ of the membrane of area A_m causes a current $J_m = A_m \rho \dot{x}$ to flow, which must pass through the weak link so that $J_s(t) = J_m$. On the other hand, $P(t)$ may be related to the stiffness k of the membrane by equating forces $kx = A_m P$, and to time evolution of the phase difference $\phi(t)$ through the ac Josephson relation $\dot{\phi}(t) = 2m_3 P/(\rho\hbar)$. Thus by measuring $x(t)$ as the membrane is driven to larger-amplitude oscillations, one obtains $J_s(t)$ by differentiation and $\phi(t)$ by integration, and then $J_s(\phi)$ by eliminating the time t. To describe the energy (or mass) storing property of the membrane one often defines a *hydrodynamic capacitance*

$$C = A_m^2 \rho^2 / k, \tag{15}$$

so that $J_m = C\dot{P}/\rho$ and the energy $F_m = C(P/\rho)^2/2$ [45]. We also note that Eq. (12) yields the differential $\mathrm{d}F_J = (\hbar/2m_3)J_s(\phi)\mathrm{d}\phi$. Therefore, if

$J_s(\phi)$ is single-valued (*i.e.*, non-hysteretic), the energy of the weak link may be obtained with

$$F_J(\phi) = \frac{\hbar}{2m_3}\int_0^\phi J_s(\phi')\mathrm{d}\phi' \tag{16}$$

up to an integration constant. By writing $\mathrm{d}F_J = L_w(\phi)J_s(\phi)\mathrm{d}J_s$, the Josephson coupling may be also described by the *hydrodynamic inductance* [45]

$$L_w(\phi) = \kappa_0/[2\pi J_s'(\phi)], \tag{17}$$

which is nonlinear in ϕ. For small ϕ the combination of C and $L_w(\phi)$ form a linear LC circuit. This means that the system can undergo harmonic oscillations around the minimum of $F_J(\phi)$ at $\phi = 0$ with the *plasma frequency* $\omega_w = 1/\sqrt{L_w(0)C}$ [47]. In Ref. [20] it was found that when this oscillator was slowly driven to larger-amplitude deviations from $\phi = 0$, it could suddenly become trapped in a state where similar stable oscillations seemed to occur around $\phi = \pi$. Thus $F_J(\phi)$ had a minimum also at this point, now known as a π *state*. In these experiments, a weak link consisting of an array of parallel apertures was used. Also measurements of the $I - P$ characteristics under a constant pressure bias have been made in the cell configuration (a) [19,22,48]. The above analysis neglected the dissipative currents, assuming them to be small.

In configuration (b) there exists an additional flow channel in parallel with the weak link, so that a closed superfluid loop may be drawn around a path containing the weak link. In an inertial frame, the circulation κ around the loop is quantized according to $\kappa = \oint \mathbf{v}_s \cdot \mathrm{d}\mathbf{r} = \kappa_0 n$, where $\kappa_0 = h/2m_3$ is the quantum of circulation in ^{3}He and n is an integer [38]. If the loop is put into rotation with the rotation field $\mathbf{\Omega}$ (typically the angular frequency of the Earth), then in the rotating frame $\mathbf{v}_s \to \tilde{\mathbf{v}}_s = \mathbf{v}_s - \mathbf{\Omega} \times \mathbf{r}$ and the circulation becomes $\tilde{\kappa} = \kappa - 2\mathbf{\Omega} \cdot \mathbf{S}_{\mathrm{loop}}$, where $\mathbf{S}_{\mathrm{loop}}$ is the directed area of the loop. There exists an analogy here with a superconductor loop placed in a magnetic field, where $2\mathbf{\Omega}$ plays the role of the field and κ that of magnetic flux. This allows the junction to be phase-biased in a controllable way [9,23]. Suppose the loop has a total length l and an effective cross-sectional area A_l. The hydrodynamic inductance L_l of the flow path is then defined as

$$L_l = l/(\rho_s A_l), \tag{18}$$

such that the kinetic energy is $F_l = L_l J_l^2/2$, where $J_l = A_l \rho_s v_s$ and v_s is the superfluid velocity. Now if the membrane is driven to oscillation with a large amplitude, then the current through the weak link may be neglected and the system of the membrane and the parallel flow path forms a classical hydrodynamic oscillator (a "Helmholtz resonator") with the natural frequency

$\omega_l = 1/\sqrt{L_l C}$. However, in general one must consider the weak link and the flow path together as a parallel combination of two inductances, with the total inductance $L(\phi) = L_w(\phi)L_l/[L_w(\phi) + L_l]$. Defining the resonance frequency $\omega = 1/\sqrt{LC}$, one finds $(\omega/\omega_l)^2 - 1 = L_l/L_w(\phi)$ and [23]

$$(2\pi L_l/\kappa_0)J_s'(\phi) = (\omega/\omega_l)^2 - 1. \tag{19}$$

Thus the derivative of $J_s(\phi)$ is directly obtained by measuring the local ϕ-dependent resonance frequency. The phase bias ϕ itself may be determined as follows. If we define $\tilde{\phi}_{\rm loop} = 2\pi(\tilde{\kappa}/\kappa_0)$ then we see that conservation of the supercurrents requires

$$(2\pi L_l/\kappa_0)J_s(\phi) = \tilde{\phi}_{\rm loop} - \phi \tag{20}$$

and a comparison of Eqs. (19) and (20) yields $\mathrm{d}\phi = (\omega_l/\omega)^2 \mathrm{d}\tilde{\phi}_{\rm loop}$. Now noting that $\tilde{\phi}_{\rm loop} = \phi_{\rm loop} - (2\pi/\kappa_0)2\mathbf{\Omega}\cdot\mathbf{S}_{\rm loop}$ where $\phi_{\rm loop} = 2\pi(\kappa/\kappa_0)$, it is seen that $\tilde{\phi}_{\rm loop}$ may be controlled by changing the flux $2\mathbf{\Omega}\cdot\mathbf{S}_{\rm loop}$ by, for example, re-orienting the cryostat. Measuring the resonance frequency ω for several angles of the cryostat then yields ϕ by integration. This first yields $J_s'(\phi)$, and then $J_s(\phi)$ by another integration [9, 23]. Using this method, π states [$J_s'(\pi) > 0$] have been observed also in a single aperture [23]. From the above discussion it follows that configuration (b) may also be used as a sensitive gyroscope, *i.e.*, a sensor of rotation [35, 36].

From a theorist's point of view it is most convenient to make calculations for very small holes in very thin membranes. However, there are several practical difficulties which complicate the creation of small enough ($\sim$ 10 nm) holes in most materials [49]. A thin membrane is also difficult to make robust enough for it would be leak-proof when a pressure bias is applied over it. This limits the $I - P$ measurements to rather low biases. Even if these difficulties may be overcome, the uncharged mass current can only be measured by mechanical means (by observing the small displacements of a membrane) which are sensitive to mechanical noise sources. This requires that if the holes are to be small, then there must be many of them to obtain a measurable current. This is the main reason for using *arrays* of apertures as the weak links in most of the experiments done at Berkeley, and more recently also in Paris and Bayreuth [50]. It has been experimentally demonstrated that such an array may work coherently enough to be described as a *single* weak link [51]. Yet, as shown in publications [P1], [P2] and [P6] of this thesis, aperture arrays also bring about new kinds of phenomena in the form of the so-called anisotextural effect.

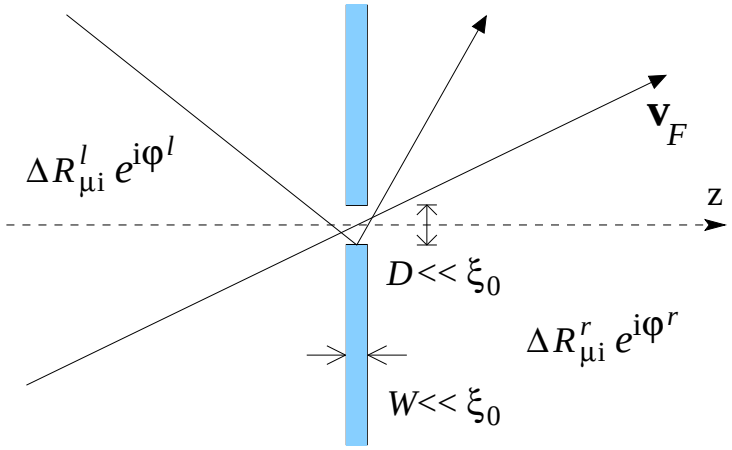

Figure 4: Two different quasiparticle trajectories through a pinhole aperture: a direct and a scattered one. The quasiparticles travel on these classical trajectories with the Fermi velocity v_F.

2 Classical point contacts

Theoretically the simplest way to describe a ^{3}He weak link is with the so-called pinhole model of a short classical point contact [15, 52, 53]. The term "pinhole" here refers to the thickness of the wall W and the diameter D of the weak link being much smaller than the zero-temperature coherence length $\xi_0 = \hbar v_F/(2\pi k_B T_c)$, see Fig. 4. This allows spatial variations inside the hole, and its feedback effects in the bulk to be neglected. "Classical" means that D is still much larger than the Fermi wavelength λ_F so that quantization of the transverse modes may be neglected. Superfluid ^{3}He is naturally pure so that the elastic mean free path $\ell \gg \xi_0$. If also $W/D \ll 1$, then quasiparticle motion through the contact is completely ballistic. For studies of the pinhole model we use the theory of quasiclassical Green's functions [42]. Adding some further simplifications, the model often makes analytical solutions possible, and below we consider some of the basic results thus obtained. Numerical calculations taking into account the gap-suppression effect of Fig. 2 are presented in publications [P2] and [P6].

2.1 Coupling energy

In publication [P2] we considered the derivation of the coupling energy of the pinhole junction in equilibrium. Often $F_J(\phi)$ is simply integrated from $J_s(\phi)$ with Eq. (16). However, the unknown integration constant may depend on

$R^{l,r}$, and therefore Eq. (16) does not necessarily give the relative energies between different $R^{l,r}$-branches correctly. This is especially important when, as in the anisotextural case to be discussed below, $R^{l,r}$ may change as a function of ϕ. In any case, it is theoretically interesting to derive the energy of the junction independently of the currents.

The derivation is very similar to the quasiclassical handling of small impurities [42]. The coupling energy is defined as the free-energy difference between an open and a closed pinhole, the role of the impurity being played by the scattering potential used for doing the closing. Apart from constant terms independent of ϕ and $R^{l,r}$, the energy is of the form [P2]

$$\begin{aligned} F_J = -\frac{\pi}{2} S\hbar v_F N(0) k_B T \sum_{\epsilon_m} \int \frac{\mathrm{d}\Omega_{\hat{\mathbf{k}}}}{4\pi} |\hat{k}_z| \\ \times \left\langle \ln \left\{ \mathrm{Det}_4 \frac{1}{2} \left[\hat{g}(\hat{\mathbf{k}}, \mathbf{0}^l, \epsilon_m) - \hat{g}(\underline{\hat{\mathbf{k}}}, \mathbf{0}^l, \epsilon_m) \right] \right\} \right\rangle , \end{aligned} \tag{21}$$

where S is the area of the pinhole and $N(0) = m^{*2} v_F/(2\pi^2\hbar^3)$ is the normal-state density of states, m^* being the effective quasiparticle mass. The 4×4 matrix $\hat{g}(\hat{\mathbf{k}}, \mathbf{R}, \epsilon_m)$ is the quasiclassical Nambu-matrix propagator [42] close to the open pinhole. It is in the Matsubara representation with the Matsubara energies $\epsilon_m = \pi k_B T(2m+1)$, $m = 0, \pm 1, \pm 2, \ldots$, and we use the normalization $\hat{g}\hat{g} = -\hat{1}$. The position $\mathbf{R} = \mathbf{0}^l$ denotes the one immediately to the left of the junction, and the reflected direction $\underline{\hat{\mathbf{k}}}$ may be chosen as $\underline{\hat{\mathbf{k}}} = -\hat{\mathbf{k}}$. The symbolic average $\langle \cdots \rangle$ is over all trajectories hitting the pinhole in direction $\hat{\mathbf{k}}$. Equation (21) is valid for any superfluid system for which the quasiclassical theory is valid, not only ^{3}He. However, in publication [P2] the energy was further simplified only in the case of a pinhole between two volumes of ^{3}He-B. It was shown that Eq. (21) is consistent with Eqs. (12) and (13) when the mass supercurrent is calculated from

$$\mathbf{j}_s(\mathbf{R}) = 2m_3 v_F N(0) \pi k_B T \sum_{\epsilon_m} \langle \hat{\mathbf{k}} \, \mathrm{Tr}\, \underline{g}(\hat{\mathbf{k}}, \mathbf{R}, \epsilon_m) \rangle_{\hat{\mathbf{k}}} / 2 \tag{22}$$

and the spin supercurrent from

$$\mathbf{j}^{sp}_\alpha(\mathbf{R}) = \hbar v_F N(0) \pi k_B T \sum_{\epsilon_m} \langle \hat{\mathbf{k}} \, \mathrm{Tr}[\underline{\sigma}_\alpha \underline{g}(\hat{\mathbf{k}}, \mathbf{R}, \epsilon_m)] \rangle_{\hat{\mathbf{k}}} / 2. \tag{23}$$

Here $\langle \cdots \rangle_{\hat{\mathbf{k}}} = \int (\mathrm{d}\Omega_{\hat{\mathbf{k}}}/4\pi)(\cdots)$ is a Fermi-surface average, and $\underline{g}$ is the "upper-left" spin matrix of $\hat{g}$ [42].

In publication [P2] we have also modeled the effect of a finite ratio W/D by simple statistical distributions for the directions of quasiparticles which

have scattered from the surface inside the contact (see Fig. 4). It was expected that this could lead to the presence of π states (minima of F_J at $\phi = \pi$) even for $R^l = R^r$, which is otherwise not possible for a single pinhole [29]. However, no significant qualitative differences to the $W/D = 0$ case were found.

2.2 Superfluid state in equilibrium

Let us now consider the equilibrium mass currents in a B-phase pinhole with $W/D = 0$. Neglecting the suppression of the order parameter, we assume Eq. (4) to be valid all the way to the wall on both (l and r) sides, and define the unit vectors $\hat{\mathbf{d}}^{l,r}(\hat{\mathbf{k}}) = R^{l,r}\hat{\mathbf{k}}$. If, for each $\hat{\mathbf{k}}$, we choose the spin quantization axis parallel to $\hat{\mathbf{d}}^l \times \hat{\mathbf{d}}^r$, the condensate may be divided into $\uparrow\uparrow$ and $\downarrow\downarrow$ parts which behave much like two independent s-wave systems [29]. Their phase differences over the contact are given by $\phi_{\hat{\mathbf{k}}.\sigma} = \phi - \sigma\chi_{\hat{\mathbf{k}}}$, where $\sigma = \pm 1$, $\phi = \varphi^r - \varphi^l$, and $\chi_{\hat{\mathbf{k}}} = \arccos(\hat{\mathbf{d}}^l \cdot \hat{\mathbf{d}}^r)$. Inside the junction, there are bound quasiparticle states whose energies depend on ϕ. As discussed in publication [P5], they are

$$\epsilon_{\hat{\mathbf{k}},\sigma}(\phi) = -\,\mathrm{Sign}(\hat{k}_z \sin(\phi_{\hat{\mathbf{k}},\sigma}/2))\Delta\cos(\phi_{\hat{\mathbf{k}},\sigma}/2), \quad \sigma = \pm 1, \tag{24}$$

where the z axis points from l to r. These states may be interpreted as carrying the supercurrent over the contact via the process of Andreev reflection [54]. The expression for the particle supercurrent is [29]

$$I(\phi) = \frac{\pi}{2} v_F \Delta N(0) S \sum_{\sigma=\pm 1} \left\langle |\hat{k}_z| \sin(\phi_{\hat{\mathbf{k}}_\sigma}/2) \tanh\left(\Delta\cos(\phi_{\hat{\mathbf{k}},\sigma}/2)/2k_BT\right)\right\rangle_{\hat{\mathbf{k}}}. \tag{25}$$

For suitably chosen matrices $R^l \neq R^r$ a cancellation between the $\hat{\mathbf{k}}$-averaged $\sin(\phi_{\hat{\mathbf{k}},\sigma})$ components of the currents for $\sigma = \pm 1$ may lead to the formation of π states [$I'(\pi) > 0$] of the type suggested by Yip [29], and even an exactly π periodic $I(\phi)$. Physically, $R^{l,r}$ may be controlled with magnetic fields, for example. These ideas have been further considered in Ref. [33].

When the suppression of the order parameter at solid surfaces (Fig. 2), is taken into account, there will be some modifications to the bound states and the current-phase relation, which can only be calculated numerically. This we have done in publications [P2] and [P6]. Figure 5 shows the bound-state peaks in the $\hat{\mathbf{k}}$-dependent density of states $N_\sigma(\hat{\mathbf{k}}, \epsilon)$ as a function of ϕ for both the $\sigma = \pm 1$ spin bands inside the junction for a one $\hat{\mathbf{k}}$ direction and temperature when $-\hat{\mathbf{n}}^l = \hat{\mathbf{n}}^r = \hat{\mathbf{z}}$. For the case with no gap suppression, the two spin-split states are simply given by Eq. (24). In the case of the diffusive wall, the numerical diagonalization of the upper-left spin matrix $\underline{g}^R(\hat{\mathbf{k}}, \epsilon)$ of

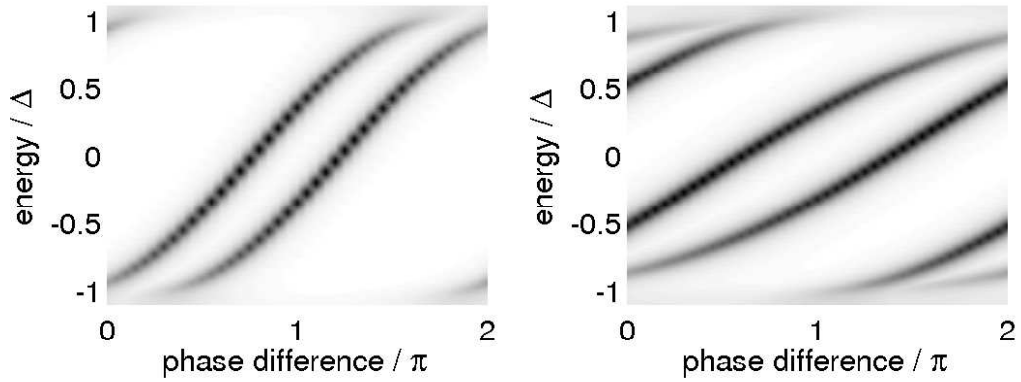

Figure 5: Bound quasiparticle states for $-\hat{\mathbf{n}}^l = \hat{\mathbf{n}}^r = \hat{\mathbf{z}}$, $\hat{k}_z = 0.93$ and $T/T_c = 0.6$, as represented by a gray-scale contour plot of the peaks in the density of states. (The width of the peaks is proportional to the inverse quasiparticle lifetime Γ, which appears as an imaginary part in energies — see below. Here it is given a large arbitrary value for purposes of illustration.) The left-hand figure corresponds to Eq. (24), and the right-hand one to the case where suppression of the order parameter has been taken into account. The states for $\sigma = 1$ ($\sigma = -1$) spin band are those shifted to the left (right) from the middle.

the retarded Nambu matrix $\hat{g}^R$ has been done for each energy separately and $N_\sigma(\hat{\mathbf{k}}, \epsilon) = -N(0)\,\mathrm{Im}\, g^R_{\sigma\sigma}(\hat{\mathbf{k}}, \epsilon)$ when the normalization $\hat{g}^R\hat{g}^R = -\hat{1}$ is used [42]. It is seen that the spin-splitting remains qualitatively similar, but the ϕ-dependence is not so steep, so that there in fact exist *two* bound states at the same time for given $\hat{\mathbf{k}}$, ϕ and σ. Also, the splitting angle is now energy-dependent.

2.3 Normal state with bias: Sharvin's conductance

Next consider two volumes of *normal* fluid ^{3}He which are connected by the same pinhole as above, but now biased by a pressure head P, or chemical potential difference $U = (m_3/\rho)P$. The particle current I through the contact is then linear in the pressure, like Ohm's law, so that $I = G_N U$, where

$$G_N = \frac{1}{2} v_F N(0) S. \tag{26}$$

The constant G_N is usually called Sharvin's conductance [55]. The current may be thought to arise from a ballistic "effusion" of the quasiparticles

coming from the l and r equilibrium distributions (see Fig. 4) close to the Fermi energy, which on one side is shifted upward by U [56]. The quantity $2v_F SN(0)U\hat{k}_z$ is the net flux of particles coming from direction $\hat{\mathbf{k}}$, and Eq. (26) follows from an average over $\hat{k}_z > 0$. Another way to arrive at this result is to use Landauer's formula for the conductance of mesoscopic contacts [57]. The conductance of each transverse mode is $2/h$ such that the total conductance is $G_N = (2/h)M$, where M is the number of conducting modes. Calculating M for the ballistic classical point contact yields $M = Sk_F^2/(4\pi)$, where $k_F = 2\pi/\lambda_F = (m^*/\hbar)v_F$, and thus Eq. (26) again follows.

2.4 Superfluid state with bias

Finally, when the pinhole in the superfluid state is biased by the chemical potential difference $U = (m_3/\rho)P$, the calculation becomes considerably more difficult. In this case there will be a dissipative dc current due to the process of *multiple Andreev reflections* (MAR), which has been thoroughly investigated in both ballistic and diffusive superconductor junctions [58–63]. In the case of superfluid ^{3}He it seems to have been systematically considered in publications [P5] and [P6] for the first time. The basic idea is that in a junction with non-tunnel conductivity also the superfluid part may contribute to the time-averaged current, since the energy of the transported Cooper pairs can be absorbed by the quasiparticles in the sub-gap bound states inside the contact, Fig. 5. For each Cooper pair, a quasiparticle performs one back-and-forth Andreev reflection, during which it gains the energy $2U$, and this happens repeatedly. This process is illustrated schematically in Fig. 2 of paper [P5]. The only way for the quasiparticle to escape from the MAR cycle is to gain enough energy to reach the gap edge after $\sim \Delta/U$ reflections, or to scatter inelastically. Whereas in superconductors the dominating inelastic process is quasiparticle-phonon scattering, for ^{3}He the only important process is quasiparticle-quasiparticle collisions. Inelastic processes are important at very low biases, since then the scattering rate Γ restricts the number of reflections to $\sim \Delta/(\hbar\Gamma)$, and thus limits the amount of current. The number of successive reflections may still be very large, and the dc currents are typically orders of magnitude larger than in the normal state with equal bias.

For a constant bias the total particle current may be expanded as [60]

$$I(P,t) = I_0(P) + \sum_{m=1}^{\infty} [I_m^C(P)\cos(m\omega_J t) + I_m^S(P)\sin(m\omega_J t)], \qquad (27)$$

where I_0 is the dc current, while I_m^C and I_m^S are the amplitudes for oscillating (super)current components. The calculation of these quantities requires the

use of quasiclassical nonequilibrium (or Keldysh) formalism [42]. For this task we use the parametrization of the Green functions with the so-called coherence functions, or Riccati amplitudes $\underline{\gamma}^{R,A}$ [64], which may be interpreted as Andreev-reflection amplitudes [62]. If we write the particle current thus obtained as

$$I(P,t) = G_N \langle |\hat{k}_z| I(\hat{\mathbf{k}},t) \rangle_{\hat{\mathbf{k}}} \tag{28}$$

and expand the T_J-periodic function $I(\hat{\mathbf{k}},t)$ in Fourier components $I(\hat{\mathbf{k}},t) = \sum_{m=-\infty}^{\infty} I_m(\hat{\mathbf{k}}) e^{\mathrm{i}m\omega_J t}$ then, neglecting gap suppression [P5]

$$\begin{aligned} I_m(\hat{\mathbf{k}}) =& 2U\delta_{m0} + 2\cos(m\chi_{\hat{\mathbf{k}}})\mathcal{P}\int_{-\infty}^{\infty} \mathrm{d}\epsilon \tanh(\epsilon/2k_BT) \\ & \times (1-|\gamma^R(\epsilon)|^2) \sum_{l=0}^{\infty} \prod_{q=1}^{l} |\gamma^R(\epsilon - qU)|^2 \prod_{p=l+1}^{l+2m} \gamma^R(\epsilon - pU). \end{aligned} \tag{29}$$

Here $\gamma^R(\epsilon) = -\Delta/(\epsilon^R + \mathrm{i}\sqrt{\Delta^2 - (\epsilon^R)^2})$, $\epsilon^R = \epsilon + \mathrm{i}(\hbar\Gamma/2)$, $\Gamma(\epsilon)$ is the relaxation rate due to quasiparticle collisions. (Their effect on $\underline{\Delta}$ is neglected.) The quantity $|\gamma^R(\epsilon)|^2$ is an Andreev-reflection probability, which is close to unity for $|\epsilon| < \Delta$, and the index l is the number of successive reflections. Equation (29) generalizes the s-wave result of Ref. [62] for the p-wave case of ^{3}He-B. From this it follows, among other things, that the I_0 current is completely independent of $R^{l,r}$.

For small biases, $U \ll \Delta$, one may also describe the current in terms of the occupation of the adiabatically moving bound states $\epsilon_{\hat{\mathbf{k}},\sigma}(\phi)$. The current may then be written as

$$I(P,t) = 4\pi G_N \sum_{\sigma,\delta=\pm1} \left\langle \hat{k}_z \frac{\mathrm{d}\epsilon_{\delta\hat{\mathbf{k}},\sigma}[\phi(t)]}{\mathrm{d}\phi} p_{\delta\hat{\mathbf{k}},\sigma}[\phi(t)] \right\rangle_{\hat{k}_z>0}, \tag{30}$$

with $\langle\cdots\rangle_{\hat{k}_z>0} = \int_{\hat{k}_z>0}(\mathrm{d}\Omega_{\hat{\mathbf{k}}}/4\pi)(\cdots)$, $\delta = \mathrm{Sign}(\hat{k}_z)$. The distribution function $p_{\hat{\mathbf{k}},\sigma}[\phi(t)]$ satisfies a kinetic equation of the form [62]

$$\frac{\mathrm{d}p_{\hat{\mathbf{k}},\sigma}[\phi(t)]}{\mathrm{d}t} = \Gamma(\epsilon)\left\{ f(\epsilon) - p_{\hat{\mathbf{k}},\sigma}[\phi(t)] \right\}, \tag{31}$$

where $f(\epsilon) = (1-\tanh(\epsilon/2k_BT))/2$ is the equilibrium Fermi distribution, and $\epsilon = \epsilon_{\hat{\mathbf{k}},\sigma}[\phi(t)]$. The boundary conditions on this equation are set by thermalization of the bound states at the gap edges [62]. In equilibrium $p_{\hat{\mathbf{k}},\sigma} = f(\epsilon)$ and Eq. (30) reduces to Eq. (25). The kinetic-equation approach is further discussed in publication [P6]. At least in principle, the gap-suppression effect of Fig. 2 may also be taken into account by replacing $\epsilon_{\hat{\mathbf{k}},\sigma}(\phi)$ with the numerically evaluated bound-state energies, see Fig. 5.

For $U \ll \hbar\Gamma$ Eq. (31) is not difficult to solve. The resulting $I - P$ curve is linear and given by

$$I_0 = g(T)\frac{\Delta}{\hbar\Gamma(0)}G_N U, \tag{32}$$

where the temperature factor $g(T) = \int_{-1}^{1} \tanh(\Delta x/2k_BT)(x/\sqrt{1-x^2})\mathrm{d}x$. At low temperature $\Delta/(\hbar\Gamma) \gg 1$ so that the slope of the $I - P$ curve is a lot steeper than in the normal state. In the experiments of Ref. [22] the condition $U \ll \hbar\Gamma$ is well satisfied, and Eq. (32) indeed accounts for the orders of magnitude of the observed currents [P5, P6]. However, Eq. (32) is not enough to explain the experiments of Ref. [22], since there the dissipative current is found to be nonlinear and to depend on the texture. Furthermore, MAR is not the only conceivable model which gives a linear current of similar magnitude [22, 65].

In publication [P6] we also report of detailed numerical calculations of the amplitudes in Eq. (27), where we take self-consistently into account the gap-suppression effect at the walls. While I_m^C and I_m^S depend strongly on $R^{l,r}$ and whether or not the gap suppression is included, the independence of I_0 on $R^{l,r}$ is approximately true also in general. The overall behavior of $I_0(P)$ is very similar to what is seen in experiments with single apertures [19], although the apertures in question did not satisfy the requirements for a pinhole. In the limit $U \ll \hbar\Gamma$ the current I_0 is also still well described by Eq. (32), where only the numerical value of $g(T)$ is slightly modified. Thus even the gap-suppression effect cannot resolve the differences between the experimental observations and the prediction of MAR theory for pinholes. To explain them, we employ the concept of anisotextural Josephson effect, explained below in Sec. 4.

In principle, the quasiparticle relaxation rate $\Gamma(\epsilon)$ could be calculated from the collisional self energy [42]. However, we always estimate its magnitude from normal-state measurements which yield $\Gamma^{-1} \sim 1\ \mu\mathrm{s}(\mathrm{mK}/T)^2$ [38]. Since the gap is suppressed close to the contact, we expect this to give a reasonable estimate also in the superfluid state, at least at the low energies which are involved when $U \ll \hbar\Gamma$.

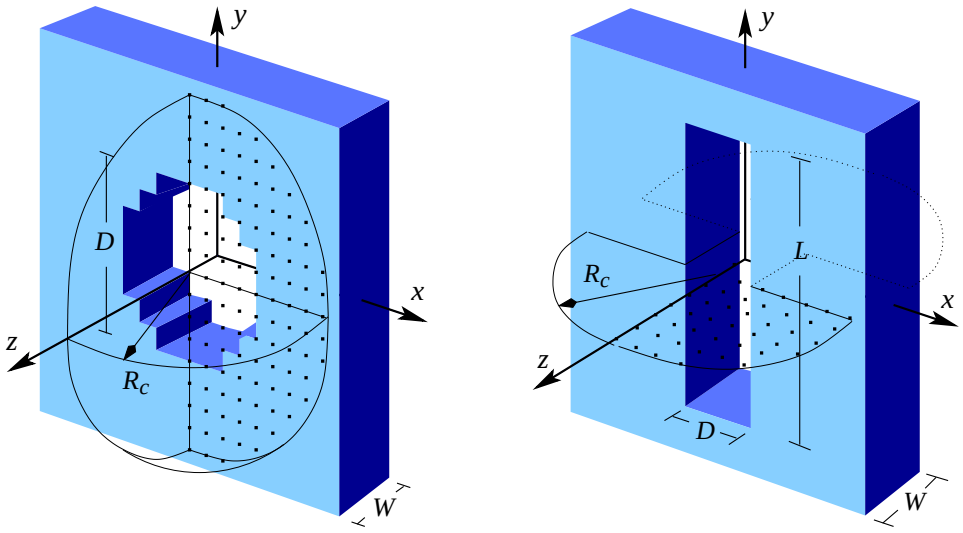

Figure 6: Calculations were made for a round aperture in 3D (left) and for a 2D model of a long slit-like aperture (right).

3 Supercurrents in large apertures

In publications [P1], [P3] and [P4] we have reported results of extensive Ginzburg-Landau (GL) simulations of stationary superflow in apertures with dimensions on the order of the GL coherence length $\xi_{GL}(T) = \hbar v_F/(\sqrt{10}\Delta)$. These represent an extension of the two-dimensional (2D) calculations reported already in Ref. [14]. However, we also carried out some fully three-dimensional (3D) simulations — the geometries are shown in Fig. 6. In the 2D simulations we studied, in addition to B phase weak links (BB), also weak links between two volumes of A phase (AA) and cases where there is A phase on one side and B phase on the other (AB). In all the BB, AA, and AB junctions the critical currents were mapped as functions of the wall thickness W and the diameter or slit width D, and phase diagrams for different types of solutions were constructed. We have always assumed all solid surfaces to be diffusely scattering, which, in the GL region ($T \approx T_c$), amounts to imposing the boundary condition $A_{\mu i} = 0$ for $\mu, i = x, y, z$ at the surfaces. Up to some cutoff around the aperture, all nine complex components $A_{\mu i}$ were allowed to vary freely in minimizing the GL energy functional [P3].

3.1 Calculations for the B phase

For publication [P1], we carried out a 3D simulation of a "round" aperture (Fig. 6) and demonstrated that there exists a solution of the GL equations

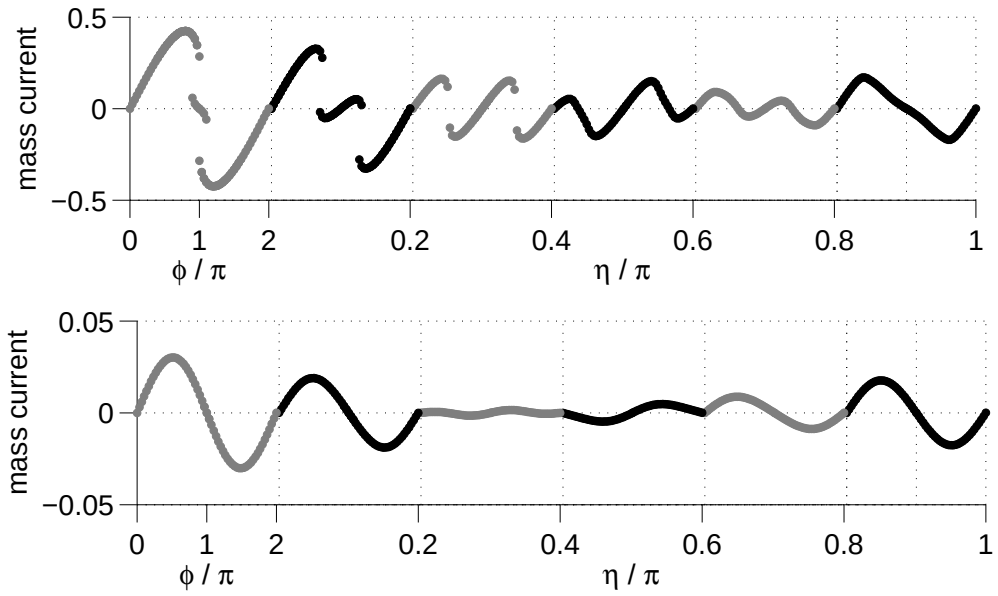

Figure 7: Current-phase relations (in arbitrary units) for two junctions with $W/\xi_{GL} = 2$ where $\hat{\mathbf{n}}^r = \hat{\mathbf{z}}$ and $\hat{\mathbf{n}}^l$ is tilted from $\hat{\mathbf{z}}$ around the y axis by angle $\eta = 0.0, 0.2\pi, \ldots, 0.8\pi$. The upper panel is for $D/\xi_{GL} = 4$ and the lower one for $D/\xi_{GL} = 2$. Hysteresis is present only in the former, where also stronger π states exist. The range of ϕ for each η is from 0 to 2π, the leftmost curves corresponding to $\eta = 0$. Here the slope of the CPR on the "π branch" for $\eta = 0$ is negative, but a positive value is possible for larger D, as in [P1].

for the phase difference $\phi = \pi$, where the current-phase relation (CPR) has a positive slope: $J_s'(\pi) > 0$. Thus this state was another example of a metastable π state, of the type observed in Ref. [20]. The solution is similar to the one inside a B-phase double-core vortex [66], so that the π state may be thought to have formed through a phase slip by a half-quantum vortex. Unlike the π states related to Eq. (25), this one could exist for parallel spin-orbit rotation axes $\hat{\mathbf{n}}^l = \hat{\mathbf{n}}^r$ [P1]. However, the calculation was restricted to the parallel case only. The CPR was found to be strongly hysteretic and the π branch was not even clearly a local minimum of the energy-phase relation at $\phi = \pi$. Thus the experimental accessibility of this π state remained questionable.

For publication [P3] we made similar calculations with a 2D model of a "slit-like" aperture, where the height L of the slit is much larger than the width D — see Fig. 6. This time we could use any rotation matrices $R^{l,r}$ as boundary conditions. Also in this case the π branch was inaccessible for

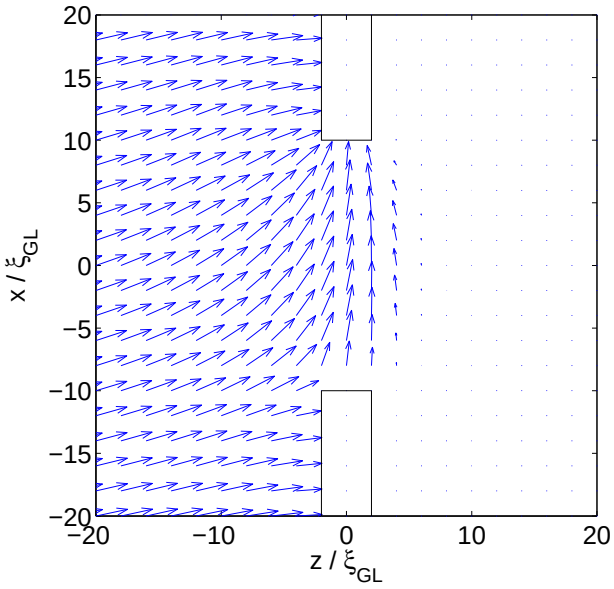

Figure 8: Example of a stable A-B phase boundary for $W/\xi_{GL} = 4$, $D/\xi_{GL} = 20$ at $p = 33$ bar. The A phase is on the left side and the B phase is on the right side. The vector field, with components $l_i = \epsilon_{ijk}\,\mathrm{Im}(A^*_{\mu j}A_{\mu k})/2\Delta_A^2$, describes the anisotropy direction $\hat{\mathbf{l}}$ of the A phase [P3]. This tends to be oriented parallel to the boundary, whose form approximates a circular arc.

$\hat{\mathbf{n}}^l = \hat{\mathbf{n}}^r$ due to hysteresis. However, it was shown that the hysteresis could be reduced by tilting the $\hat{\mathbf{n}}^{l,r}$ slightly from the parallel configuration. In this way the π branch of [P1] could be made stable and accessible in principle, as shown in Fig. 7. It was shown that the CPR's tended to be hysteretic and with strong π-branches for $D/\xi_{GL} \gtrsim 3$ and non-hysteretic for $D/\xi_{GL} \lesssim 3$. The value $D/\xi_{GL} \approx 3$ roughly coincides with the critical separation π for the destruction of superfluidity in a parallel-plate geometry with diffusive surfaces [67]. Various boundary conditions using an external magnetic field to control $\hat{\mathbf{n}}^{l,r}$ were also tested to show that similar π states should exist also under experimentally achievable conditions. In [P3] we also calculated Josephson spin currents in addition to the mass currents, and discussed their connection to the π states.

3.2 The A phase and pinned A-B boundaries

In publication [P3] we also reported 2D calculations of CPR's for the slit-like weak links when the AA or AB phase combinations are present. In

the latter case a phase boundary between the A and B phases is formed inside the aperture [68]. However, this boundary is only stable under certain conditions close to the A-B coexistence point, which, experimentally, is at pressure $p \approx 21$ bar in the GL regime (see Fig. 1). This stability was studied numerically in publication [P4]. For a wide slit of width D the stability condition may be written with the surface tension σ_{AB} and the difference between bulk condensation energies $\Delta f_{AB} = f_A - f_B$ as [69]

$$|\Delta f_{AB}| < \frac{\sigma_{AB}}{D}. \tag{33}$$

The A phase is stabilized relative to the B phase at high pressures by the so-called strong-coupling effects [42]. We took these into account with the Sauls-Serene corrections to the GL parameters [70], which give the coexistence pressure ($\Delta f_{AB} = 0$) at roughly $p = 28.7$ bar. Using the condition (33) we evaluated σ_{AB} by increasing $|f_{AB}|$ with pressure until the interface became unstable and "popped" out of the aperture. Figure 8 shows an example of a bulging phase boundary at high pressure, where the A phase is more stable. Equation (33) assumes the radius of curvature and σ_{AB} to be constants over the boundary — the effect of the non-uniform $\hat{\mathbf{l}}$-field on these assumptions was not studied in detail. However, the value $\sigma_{AB} \approx 0.93 \xi_{GL} f_B$ obtained in this way is in agreement with direct calculations for a planar A-B interface [71], and our method is closer to the way in which it has been measured in experiments [69].

Experiments on the Josephson effects involving the A phase have not been made so far, but our calculations give predictions for the kind of phenomena to be expected. In particular, in both the AA and AB cases there exist many solutions where the $\hat{\mathbf{l}}$ texture is different inside the aperture, and since $\hat{\mathbf{l}}$ is coupled to the superflow, transitions between different $\hat{\mathbf{l}}$ configurations may occur, which give hysteretic jumps in the CPR. It should be noted that the A phase junction considered as a pinhole contact would not be as interesting, since for antiparallel $\hat{\mathbf{l}}$'s on the two sides ($-\hat{\mathbf{l}}^l = \hat{\mathbf{l}}^r = \hat{\mathbf{z}}$) the critical current vanishes identically due to symmetry reasons. The same is true for large apertures with continuous rotation symmetry around the z axis, like the round aperture of Fig. 6, since the junction may continuously unwind the phase difference ϕ by rotating the $\hat{\mathbf{l}}$ texture. Thus in general the phase difference itself is not even well defined in the case of A phase. However, for less symmetrical apertures where $\hat{\mathbf{l}}$ is fixed, a finite critical current is possible even in the antiparallel case. For example, in the AA case with $\hat{\mathbf{l}}^{l,r} = \pm\hat{\mathbf{z}}$ on the two sides of the slit of Fig. 6, the vector $\hat{\mathbf{l}}$ is approximately confined to the xz plane everywhere, and ϕ is a well-defined quantity.

4 The anisotextural effect

The coupling of the phase and spin-orbit degrees of freedom described by Eq. (11) has significant consequences in restricted geometries where the $\hat{\mathbf{n}}$ texture is not rigidly fixed [by F_{SD} in Eq. (9), for example] and hence $F_J(\phi, \psi_{ij})$ is the dominant $\hat{\mathbf{n}}$-dependent contribution to the total free energy. In such a case, when the phase ϕ is swept slowly by applying a small pressure head across the weak link, ψ_{ij} will tend to follow the local equilibrium configuration which depends on ϕ. This yields strongly non-sinusoidal current-phase relations where it is possible to have $J_s'(\phi) > 0$, *i.e.*, minima of $F_J(\phi)$, at both $\phi = 0$ and $\phi = \pi$ simultaneously. The additional minima at $\phi = \pi$ are again called π *states* [20]. We have called this way of obtaining π states the *anisotextural Josephson effect* to clearly separate it from the usual *isotextural* case where the $\hat{\mathbf{n}}$ texture is fixed. We note that here the term π state differs essentially from the term "π junction" which also appears in the literature (sometimes with the name π state) and refers to a sine-like $J_s(\phi)$ which is phase-shifted by π [28]. This, too, is possible in ^{3}He-B, but it belongs to the isotextural variety of phenomena.

In publications [P1], [P2] and [P6] we considered the Berkeley experiments [20–22], where the weak link consisted of a 65×65 rectangular array of roughly 100 nm apertures in a 50 nm thick SiN membrane with a hole spacing of 3 μm. Since the macroscopic texture may be expected to play a role in the behavior of the weak link, it is important to be aware of the geometrical details of the experimental cell. This is shown in Fig. 16 of paper [P2]. The anisotextural effect should be suppressed in a strong magnetic field, since the field generally fixes the texture [P2]. This is one of the main predictions of our theory which can be tested. In the experiments of Refs. [20–22] the magnitudes of any stray fields were not well known, and we have assumed them to be negligible.

4.1 Stationary model: π states

To demonstrate the anisotextural Josephson effect it is sufficient to consider the following "tunneling" model for the coupling energy

$$F_J = -[\alpha R^l_{\mu z} R^r_{\mu z} + \beta (R^l_{\mu x} R^r_{\mu x} + R^l_{\mu y} R^r_{\mu y})] \cos\phi, \tag{34}$$

where the weak link is in a wall in the xy plane. This form is valid for temperatures $T \approx T_c$ [P1]. In the case of an array-type weak link, ϕ and ψ_{ij} are assumed to be uniform over the array, such that Eq. (34) is still valid. The two parameters $\alpha(T)$ and $\beta(T)$ may be calculated from quasiclassical

theory. They are plotted in Fig. 3 of publication [P2] for the Berkeley array, assuming all of the holes to be pinholes in a microscopically rough wall.

The purest example of the anisotextural effect could be realized by placing the weak link between two exactly spherical small containers, so that the $\hat{\mathbf{n}}$-vectors on both sides are free to orient themselves in any direction. In this case a local minimization of Eq. (34) for $\alpha < \beta$ leads to $\hat{\mathbf{n}}^l = \hat{\mathbf{n}}^r$ for $\cos\phi > 0$, and to $\hat{\mathbf{n}}^{l,r} = (\mp\hat{\mathbf{x}} + \hat{\mathbf{y}} \mp \sqrt{3}\hat{\mathbf{z}})/\sqrt{5}$ for $\cos\phi < 0$. These minima lead to the following piecewise sinusoidal current-phase relation with a π state present

$$J_s(\phi) = \begin{cases} (2m_3/\hbar)(\alpha + 2\beta)\sin\phi, & \text{for } \cos\phi > 0 \\ (2m_3/\hbar)(\alpha - 2\beta)\sin\phi, & \text{for } \cos\phi < 0. \end{cases} \tag{35}$$

The second simplest case is to have an aperture array in an infinite planar wall with normal $\hat{\mathbf{z}}$. Then the most natural configuration for $\hat{\mathbf{n}}^{l,r}$ is to be along $\pm\hat{\mathbf{z}}$, which corresponds to the minimum of the surface-dipole energy F_{SD}. For the weak link this yields *two* non-equivalent but degenerate configurations, where the $\hat{\mathbf{n}}'s$ are either parallel ($\hat{\mathbf{n}}^l = \hat{\mathbf{n}}^r = \pm\hat{\mathbf{z}}$) or antiparallel ($-\hat{\mathbf{n}}^l = \hat{\mathbf{n}}^r = \pm\hat{\mathbf{z}}$). However, the actual ϕ-dependent texture close to the weak link is determined by a competition between F_J, F_G, and F_{SD}, which poses a complicated numerical problem. Thus, in order to analyze more realistic geometries, we make several simplifying assumptions.

First, as seen in Fig. 16 of publication [P2] which describes the Berkeley cell, it is a reasonably good assumption to take the texture on one side of the weak link to be fixed by F_{SD} — we choose $\hat{\mathbf{n}}^r = \hat{\mathbf{z}}$. On the other side the texture is much more susceptible to perturbations, and the orienting effect of F_{SD} is small compared to that of F_J [P2]. Second, we estimate the energies with simple models where the l-side texture is described only by its angle $\eta(r)$ with respect to $\hat{\mathbf{z}}$, which depends on the radial distance r from the weak link. A cutoff is chosen at $r = R_0 = \sqrt{S_{\rm tot}/\pi}$ where $S_{\rm tot}$ is the total area of the array. We also define $\eta_\infty = \eta(\infty)$ and $\eta_0 = \eta(R_0)$. The purely parallel and antiparallel configurations are achieved by $\eta_\infty = 0$ and π, respectively. However, the existence of exactly two almost degenerate textural configurations is true also in general, regardless the left-side geometry. Thus we allow more general values $\eta_\infty^{(1,2)}$ for the two almost degenerate cases, which satisfy $\eta_\infty^{(2)} = \pi - \eta_\infty^{(1)}$ when rotational symmetry around the z axis is assumed. The total free energy $F \approx F_J + F_G$ is now estimated with

$$F[\eta] = F_J(\eta_0, \phi) + \frac{K}{2}\int \mathrm{d}^3 r |\nabla\eta|^2, \tag{36}$$

where $K = (50/3)\lambda_{G2}$, and λ_{G2} is the gradient-energy parameter of Ref. [43].

In equilibrium, this may be written as

$$F(\eta_0, \eta_\infty, \phi) = F_J(\eta_0, \phi) + \gamma(\eta_0 - \eta_\infty)^2, \tag{37}$$

where $\gamma(T) = \pi K R_0$ and integration over the entire left half-space is assumed. An estimate which better suits the geometry of Ref. [21] is obtained by adding a factor ≈ 0.31 to γ [P2]. The anisotextural model now consists of minimizing Eq. (37) with respect to η_0 for given ϕ and η_∞.

If $\gamma \gg \alpha, \beta$ then the texture is so rigid that there occurs no variation at all when the phase is swept from 0 to 2π. In this limit, which is valid at least very close to T_c, the Josephson effect reduces to the usual, isotextural one. Toward lower temperatures $\alpha(T), \beta(T) \sim (1 - T/T_c)^2$ grow faster than $\gamma(T) \sim 1 - T/T_c$. Thus at $T \ll T_c$ there will be some textural variation and possibly formation of anisotextural π states. This is in agreement with experimental findings [20]. The fact that two different sets of CPR's (the "H" and "L" states [21]) were measured is also well explained by the superfluid choosing randomly between one of the two almost degenerate textural states at different times of cooling below T_c.

The above analysis (or that of publication [P2]) only describes the quasi-equilibrium states of the weak link for given ϕ, but neglects the way in which the equilibrium states are reached. Thus it assumes a very slow variation of ϕ and no real dynamics is involved. The problem of textural relaxation is a very complicated one, and we have not attempted to incorporate it into the model. However, as we argue below, the dynamics of the texture provides a way to dissipate energy and therefore also a mechanism for the junction to become trapped in one of the anisotextural π states.

4.2 Dynamical model: spin-wave radiation

The interest for studying the dynamics of the texture arose from the experiments of Ref. [22], where the current-pressure ($I - P$) curves of the same Berkeley weak link array were measured in the regime $U \ll \hbar\Gamma$. The observed dissipative currents could not be due to multiple Andreev reflections alone, since then the $I - P$ curves should have been strictly linear and texture-independent, as given by Eq. (32). Instead, different $I - P$ curves were measured for the H and L states, and in the H state they were strongly nonlinear. In publication [P6] we attempt to explain the texture-dependence and the nonlinearity based on the anisotextural effect. The point here is that the ability of the $\hat{\mathbf{n}}$ texture to move opens up another channel for the condensate to dissipate energy, besides the MAR process. This channel is *radiation by spin waves*.

The starting point in the analysis is Leggett's theory for spin dynamics [41], which may also be augmented with dissipative processes, such as Leggett-Takagi (LT) relaxation [72] and spin diffusion [41]. We only consider the first of these here. To this end, the total spin polarization $\mathbf{S}$ is divided into condensate and quasiparticle parts $\mathbf{S}_p$ and $\mathbf{S}_q$, respectively, which satisfy $\mathbf{S}_p = \lambda(T)\mathbf{S}$ in equilibrium. LT relaxation refers to a decay of nonequilibrium differences $\boldsymbol{\eta} = \mathbf{S}_p - \lambda\mathbf{S}$ to zero on a time scale $\tau_{LT} \sim \Gamma^{-1}$ via $\mathbf{S}$-conserving collision processes which redistribute the numbers of Cooper pairs and quasiparticles. The set of dynamical equations including this process is [72]

$$\begin{aligned}
\dot{\mathbf{S}} &= \gamma_g \mathbf{S} \times \mathbf{B} + \mathbf{R}[\hat{\mathbf{d}}] \\
\dot{\boldsymbol{\eta}} &= \gamma_g \boldsymbol{\eta} \times (\mathbf{B} - \mu_0 \gamma_g F_0^a \chi_{0N}^{-1} \mathbf{S}) + (1-\lambda)\mathbf{R}[\hat{\mathbf{d}}] - \boldsymbol{\eta}/\tau_{LT} \\
\dot{\hat{\mathbf{d}}} &= \gamma_g \hat{\mathbf{d}} \times \{\mathbf{B} - \mu_0 \gamma_g \chi^{-1}[\mathbf{S} + \lambda^{-1}(\chi/\chi_0)\boldsymbol{\eta}]\}.
\end{aligned} \tag{38}$$

Here $\hat{\mathbf{d}}(\hat{\mathbf{k}}) = R(\hat{\mathbf{n}}, \theta)\hat{\mathbf{k}}$, $\mathbf{H} = \mathbf{B}/\mu_0$ is the magnetic field, μ_0 the vacuum permeability, γ_g the gyromagnetic ratio, $\chi = \chi_0/[1 + F_0^a(\chi_0/\chi_{0N})]$ and χ_0 the spin susceptibilities with and without Fermi-liquid corrections, and χ_{0N} is the normal-state value of χ_0. The quantity $\mathbf{R}[\hat{\mathbf{d}}] = -\langle \hat{\mathbf{d}} \times (\delta F/\delta \hat{\mathbf{d}}) \rangle_{\hat{\mathbf{k}}}$ is the torque acting on $\hat{\mathbf{d}}$. The reactive terms in these equations may be derived as the canonical equations for an effective Hamiltonian $F[\mathbf{S}_q, \mathbf{S}_p, \hat{\mathbf{d}}]$ where $\mathbf{S}_q$ and $\mathbf{S}_p$ are considered as independent variables which are canonically conjugate to infinitesimal rotations in their respective spin spaces — see Ref. [72]. Assuming $\mathbf{B} = 0$, $\mathbf{S}_p || \mathbf{S}$, restricting to the hydrodynamic limit $\omega_J \tau_{LT} \ll 1$, and considering only infinitesimal rotations $\hat{\mathbf{d}} \to \hat{\mathbf{d}} + \boldsymbol{\theta} \times \hat{\mathbf{d}}$, Eqs. (38) simplify into

$$\ddot{\boldsymbol{\theta}} = \mu_0 \gamma_g^2 \chi^{-1}[\mathbf{R}(\boldsymbol{\theta}) + \tau_x \dot{\mathbf{R}}(\boldsymbol{\theta})], \tag{39}$$

where $\mathbf{R}(\boldsymbol{\theta}) = -\delta F/\delta \boldsymbol{\theta}$ and $\tau_x = [(1-\lambda)\chi/(\lambda\chi_0)]\tau_{LT}$.

Oscillations of the rotation axis. — We now return to the model of Eq. (36) used already in the stationary case, which provides the $\hat{\mathbf{d}}$-dependent terms in the effective Hamiltonian. Using the relation $\epsilon_{ijk} R_{jl} R_{km} = R_{in} \epsilon_{nlm}$ and assuming $\theta = \theta_L$, it may be shown that small deviations $\vartheta = \eta - \eta_\infty$ of a nearly uniform $\hat{\mathbf{n}}$ may be related to the infinitesimal rotation angle $|\boldsymbol{\theta}|$ by $|\boldsymbol{\theta}| = \sqrt{5/2}\vartheta$. Neglecting the LT relaxation term (*i.e.*, taking $\tau_x = 0$), the bulk part of Eq. (39) becomes a simple wave equation

$$\ddot{\vartheta} = c_{sw}^2 \nabla^2 \vartheta, \tag{40}$$

where $c_{sw} = \sqrt{2\mu_0 \gamma_g^2 K/(5\chi)}$. We also linearize $F_J \approx -[E_J^\infty - J_{sp}\vartheta_0]\cos(\phi)$, where $\vartheta_0 = \vartheta(R_0)$ and the corresponding torque term yields the boundary

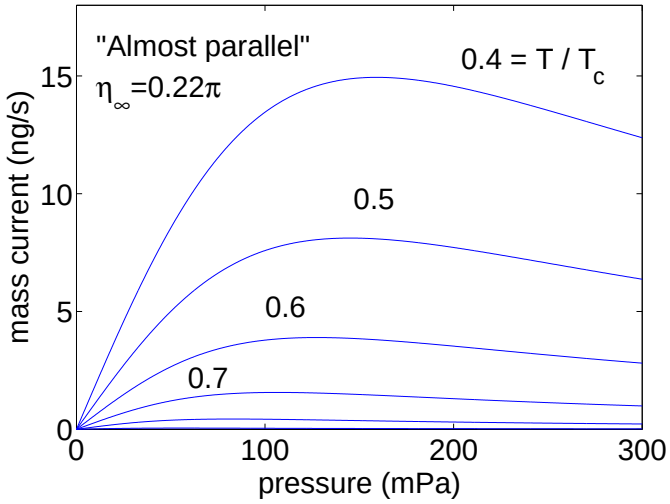

Figure 9: Current-pressure curves computed from Eq. (42), where $\eta_\infty = 0.22\pi$ and γ is multiplied by 0.31. Other parameters are as in Ref. [21].

condition

$$2\pi R_0^2 K \vartheta'(R_0) = J_{sp} \cos\phi. \tag{41}$$

This describes conservation of the component of spin current which acts to rotate $\hat{\mathbf{n}}$. If the junction is now biased with a pressure head P, then ϕ evolves according to $\phi(t) = \omega_J t$, where $\omega_J = 2m_3 P/(\rho\hbar)$. The Josephson spin current $J_{sp}\cos\phi$ will then drive oscillations of the spin polarization close to the junction. These oscillations radiate out as *spin waves*, as described by the radially outward propagating solution of Eq. (40). This radiation is associated with a phase shift between the oscillations of the driving spin current $J_{sp}\cos\phi(t)$ and of $\vartheta_0(t)$, and thus the latter obtains a component proportional to $\sin\phi$. As a result, the mass supercurrent $J_s \approx (2m_3/\hbar)(E_J^\infty - J_{sp}\vartheta_0)\sin\phi$ has a finite time average. If we also include the LT relaxation term of Eq. (39), the time average is

$$J_{s,\mathrm{ave}}(P) = \frac{2m_3}{\hbar}\frac{[J_{sp}(\eta_\infty)]^2}{4\gamma}\,\mathrm{Im}\left(\frac{1}{1+qR_0}\right), \tag{42}$$

where $q = -\mathrm{i}\omega_J/(c_{sw}\sqrt{1-\mathrm{i}\omega_J\tau_x})$. In the low-bias regime of Ref. [22] the effect of LT relaxation is negligibly small, and Eq. (42) reduces to the result of paper [P6]. Some example curves for the Berkeley array are shown in Fig. 9. Note that the linearization of F_J assumed small deviations ϑ and thus $\alpha, \beta \ll \gamma$. This is valid only for T close to T_c, as is Eq. (34) itself. Therefore, only weak anisotextural "π states" are involved here. However,

some corrections can be expected if the crude model of Eq. (36) is generalized to include more degrees of freedom.

The most important point to note in Eq. (42) is that it depends on the textural configuration through the angle η_∞ which determines the amplitude J_{sp} that drives the oscillations. We suggest that this is why the H and L states of the Berkeley experiment can have so different $I - P$ curves. It should be stressed that for this point it is essential to use one of the self-consistent surface models, since J_{sp} depends sensitively on the relative values of α and β [P6]. In view of Eq. (27), the result (42) corresponds to a finite time-average of the $I_1^S \sin(\omega_J t)$ term. Thus the total dc mass current through the weak link should be written as

$$J_{dc}(P) = J_0(P) + J_{s,\mathrm{ave}}(P), \tag{43}$$

where J_0 is the texture-independent dc part of Eq. (32) due to multiple Andreev reflections. The comparison of Eq. (43) to the Berkeley experiments, which necessarily involves the use of K, η_∞, and Γ as fitting parameters, is done in publication [P6]. An order-of-magnitude agreement is achieved.

Oscillations of the rotation angle. — Above we took the angles $\theta^{l,r}$ in $R(\hat{\mathbf{n}}^{l,r}, \theta^{l,r})$ to be fixed to $\theta_L = 104°$ which minimizes F_D in Eq. (10), while allowing the $\hat{\mathbf{n}}$ texture to bend. This relied on the assumption that in the geometry of the Berkeley cell, it is energetically less costly to let $\hat{\mathbf{n}}$ bend than to change θ: the former is associated with a relatively small cost in F_{SD}, but latter costs a considerable amount of F_D. In general, one should consider the variations of both $\hat{\mathbf{n}}$ and θ simultaneously. However, for simplicity we take only one example of the opposite case, where $\hat{\mathbf{n}}$ is fixed but the angles $\theta^{l,r}$ are allowed to vary. We choose the antiparallel configuration $-\hat{\mathbf{n}}^l = \hat{\mathbf{n}}^r = \hat{\mathbf{z}}$. In this case there is a spin current $J_z^{sp}(\phi) = \beta\sqrt{15/16}\cos\phi$ flowing though the weak link. At low frequencies the resulting shifts of $\theta^{l,r}$ from θ_L are small and restricted to distances closer to the contact than the dipole length $\xi_D = \sqrt{\lambda_{G2}/(g_D\Delta^2)} \approx 10$ μm [43]. However, when the Josephson frequency ω_J reaches the longitudinal resonance frequency $\Omega_{||} = 15\mu_0\gamma_g^2\Delta^2 g_D/\chi$, then the deviations of $\theta^{l,r}$ will also begin to propagate. This may again be described by starting from Eq. (39), where now $F = F_D + F_G$, and $\theta^{l,r} = \theta^{l,r}(z,t)$. A calculation similar to the one leading to Eq. (42) shows that there will be a net current

$$J_{s,\mathrm{ave}}(P) = \frac{2m_3}{\hbar}\frac{15}{16}\beta^2\frac{1}{2\lambda_{G2}S_{\mathrm{tot}}}\,\mathrm{Im}\,\frac{1}{q}, \tag{44}$$

where $q^2 = (15/2)(\xi_D)^{-2}[1-(\omega_J/\Omega_{||})^2/(1-\mathrm{i}\omega_J\tau_x)]$. Some of these curves are plotted in Fig. 10 for parameters taken from the Berkeley experiments. The current is very small for $\omega_J < \Omega_{||}$, after which it peaks rapidly. These peaks

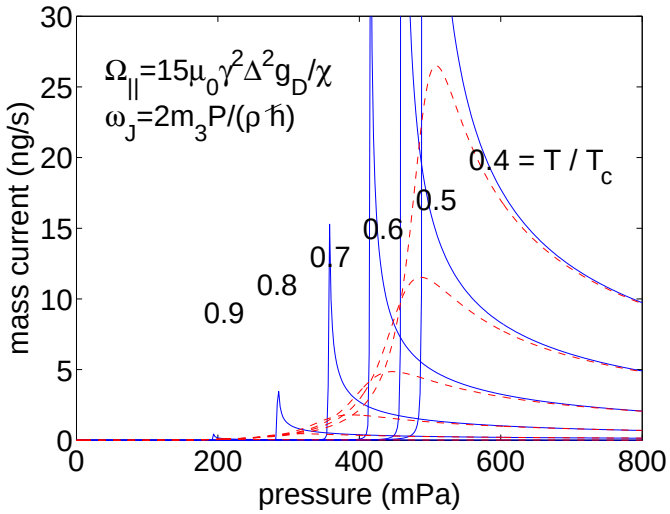

Figure 10: Current peaks due to a resonance of the Josephson frequency ω_J with the frequency $\Omega_{||}$ of the B-phase longitudinal mode. The solid lines neglect LT relaxation, while in the dashed lines it is included.

should again be added on the background current $J_0(P)$ of Eq. (43), whose magnitude is comparable to the heights of the peaks themselves. In general, small current peaks may also be expected at the "subharmonic" frequencies $\omega_J = \Omega_{||}/n$, where n is a positive integer. These are due to the presence of higher harmonics in Eq. (27), which have neglected here. The bias regime needed to observe the peaks should be within the reach of experimental techniques. However, this requires that the antiparallel configuration can be rigidly maintained. Simultaneous oscillations of $\hat{\mathbf{n}}$ and θ may smooth the peaks beyond practical observability.

Finally it should be noted how the LT relaxation effect played only a minor role in both of the radiative effects which result in the dc currents of Eqs. (42) and (44). We may thus conclude that radiation by wave motion is a much more efficient way to dissipate energy in these systems than the "diffusive" processes involving quasiparticle collisions.

5 Conclusion

In this overview we have discussed a number of published articles which represent original theoretical research on superfluid ^{3}He. Although all of the work concentrates on ^{3}He weak links alone, the range of used methods and problem types is relatively wide. Both analytical and heavily numerical calculations were carried out, whichever type of solution best suited the particular problem at hand.

All of the research was inspired by a need to explain experimental results. In addition, several predictions for testing the theories and for thus far unobserved phenomena have been presented. A large part of the work concentrated on an analysis of the so-called π states. Three different mechanisms for them have been discussed here. (Also a fourth type of suggestion has been made elsewhere [30, 31].) First, for small pinholes there exist π states of the type suggested by Yip [29, 33], due to the higher-order supercurrent harmonics in Eq. (25). Second, in larger apertures a solution of the GL equations was found which also corresponds to a π state. Finally, in array-type weak links a π state may occur when the textural configuration changes on a macroscopic scale. We called this an "anisotextural" effect. We analyzed the experiments of Refs. [20, 21] in array-type weak links and interpreted the observed π states as arising from an effect of the latter type. The "H" and "L" states seen in the experiments were interpreted as two different, almost degenerate textural states. The anisotextural effect was later used to analyze the results of Ref. [22] on the texture-dependent dissipative currents in the same experimental cell.

Despite the reasonably good agreement between the anisotextural theory and the Berkeley experiments, no "direct" observations of the anisotextural effect have been made. Therefore, their existence in the Berkeley cell remains open. Nevertheless, they are real effects, and should certainly exist in properly designed geometries. One way of direct observation would be to measure the spin-wave radiation from a pressure-biased weak link. The π states observed for single apertures in the experiments reported in Ref. [23], on the other hand, are probably due to one of the other two π-state mechanisms (or some combination). However, in this case quantitative comparison between theory and available experimental data has proved difficult. It will be interesting to see if further experiments are able to confirm the predictions which follow from our theoretical analysis. We also hope that our work will inspire research to find similar effects in weak links of unconventional superconductors, as well as in other Josephson-coupled systems where the condensates have internal degrees of freedom.

References

[1] B. D. Jopsephson, Phys. Lett. **1**, 251 (1962).

[2] K. K. Likharev, Rev. Mod. Phys. **51**, 101 (1979).

[3] M. Tinkham, *Introduction to superconductivity, 2nd ed.* (McGraw-Hill, Singapore, 1996).

[4] P. W. Anderson, Rev. Mod. Phys. **38**, 298 (1966).

[5] A. Smerzi, S. Fantoni, S. Giovanazzi, and S. R. Shenoy, Phys. Rev. Lett. **79**, 4950 (1997).

[6] O. Avenel and E. Varoquaux, Phys. Rev. Lett. **55**, 2704 (1985).

[7] O. Avenel and E. Varoquaux, Jpn. J. Appl. Phys. **26**, 1798 (1987).

[8] O. Avenel and E. Varoquaux, Phys. Rev. Lett. **60**, 416 (1988).

[9] K. Sukhatme, Yu. Mukharsky, T. Chui, and D. Pearson, Nature **41**, 280 (2001).

[10] H. Monien and L. Tewordt, J. Low. Temp. Phys **62**, 277 (1985).

[11] N. B. Kopnin, Pis'ma Zh. Eksp. Teor. Fiz. **43**, 541 (1986), [JETP Lett. **43**, 700-703 (1986)].

[12] J. R. Hook, Jpn. J. Appl. Phys. **26**, 159 (1987).

[13] S. Ullah and A. L. Fetter, Phys. Rev. B **39**, 4186 (1989).

[14] E. V. Thuneberg, Europhys. Lett. **7**, 441 (1988).

[15] J. Kurkijärvi, Phys. Rev. B **38**, 11184 (1988).

[16] E. V. Thuneberg, J. Kurkijärvi, and J. A. Sauls, Physica B **165 & 166**, 755 (1990).

[17] N. B. Kopnin, P. I. Soininen, and M. M. Salomaa, Phys. Rev. B **45**, 5491 (1992).

[18] P. I. Soininen, N. B. Kopnin, and M. M. Salomaa, Europhys. Lett. **17**, 429 (1992).

[19] J. Steinhauer, K. Schawab, Yu. M. Mukharsky, J. C. Davis, and R. E. Packard, Physica B **194-196**, 767 (1994).

[20] S. Backhaus, S. Pereverzev, R. W. Simmonds, A. Loshak, J. C. Davis, and R. E. Packard, Nature **392**, 687 (1998).

[21] A. Marchenkov, R. W. Simmonds, S. Backhaus, A. Loshak, J. C. Davis, and R. E. Packard, Phys. Rev. Lett. **83**, 3860 (1999).

[22] R. W. Simmonds, A. Marchenkov, S. Vitale, J. C. Davis, and R. E. Packard, Phys. Rev. Lett. **84**, 6062 (2000).

[23] O. Avenel, Yu. Mukharsky, and E. Varoquaux, Physica B **280**, 130 (2000).

[24] S.-K. Yip, J. Low Temp. Phys. **109**, 547 (1997).

[25] M. Fogelström, S.-K. Yip, and J. Kurkijärvi, Physica C **294**, 301 (1998).

[26] E. Il'ichev, V. Zakosarenko, R. P. J. IJsselsteijn, H. E. Hoenig, V. Schultze, H.-G. Meyer, M. Grajacar, and R. Hlubina, Phys. Rev. B **60**, 3096 (1999).

[27] M. Fogelström, Phys. Rev. B **62**, 11812 (2000).

[28] J. J. A. Baselmans, B. J. van Wees, and T. M. Klapwijk, Phys. Rev. B **65**, 224513 (2002).

[29] S.-K. Yip, Phys. Rev. Lett. **83**, 3864 (1999).

[30] N. Hatakenaka, Phys. Rev. Lett. **81**, 3753 (1998).

[31] A. Smerzi, S. Raghavan, S. Fantoni, and S. R. Shenoy, Eur. Phys. J. B **24**, 431 (2001).

[32] W. Zhang and Z. D. Wang, Phys. Rev. B **64**, 214501 (2001).

[33] M. Nishida, N. Hatakenaka, and S. Kurihara, Phys. Rev. Lett. **88**, 145302 (2002).

[34] O. Avenel, Yu. Mukharsky, and E. Varoquaux, Nature **397**, 484 (1999).

[35] O. Avenel, P. Hakonen, and E. Varoquaux, Phys. Rev. Lett. **78**, 3602 (1997).

[36] K. Schwab, N. Bruckner, and R. E. Packard, Nature **386**, 585 (1997).

[37] P. Nozieres and D. Pines, *The Theroy of Quantum Liquids* (Perseus Books, Cambridge, Massachusetts, 1996).

[38] D. Vollhardt and P. Wölfle, *The Superfluid Phases of Helium 3* (Taylor and Francis, London, 1990).

[39] V. Ambegaokar, P. G. deGennes, and D. Rainer, Phys. Rev. A **9**, 2676 (1974), Erratum: Phys. Rev. A **12**, 345 (1975).

[40] L. J. Buchholtz and D. Rainer, Z. Phys B **35**, 151 (1979).

[41] A. J. Leggett, Rev. Mod. Phys. **47**, 331 (1975).

[42] J. W. Serene and D. Rainer, Phys. Rep. **101**, 221 (1983).

[43] E. V. Thuneberg, J. Low Temp. Phys. **122**, 657 (2001).

[44] E. Zhao, T. Löfwander, and J. A. Sauls, Phys. Rev. Lett. **91**, 077003 (2003).

[45] J. C. Davis and R. E. Packard, Rev. Mod. Phys. **74**, 741 (2002).

[46] O. V. Lounasmaa, M. T. Manninen, S. A. Nenonen, J. P. Pekola, R. G. Sharma, and M. S. Tagirov, Phys. Rev. B **28**, 6536 (1983).

[47] A. Marchenkov, R. W. Simmonds, J. C. Davis, and R. E. Packard, Phys. Rev. B **61**, 4196 (2000).

[48] S. Backhaus and R. Packard, Czechoslovak Journal of Physics **46**, 2743 (1996).

[49] S. V. Pereverzev, J. Low Temp. Phys. **101**, 573 (1995).

[50] S. V. Pereverzev and G. Eska, J. Low Temp. Phys. **134**, 725 (2004).

[51] S. V. Pereverzev, A. Loshak, S. Backhaus, J. C. Davis, and R. E. Packard, Nature **388**, 449 (1997).

[52] I. O. Kulik and A. N. Omel'yanchuk, Fiz. Nizk. Temp. **3**, 945 (1977), [Sov. J. Low Temp. Phys. **3**, 459-461 (1978)].

[53] I. O. Kulik and A. N. Omel'yanchuk, Fiz. Nizk. Temp. **4**, 296 (1978), [Sov. J. Low Temp. Phys. **4**, 142-149 (1978)].

[54] A. M. Zagoskin, *Quantum Theory of Many-Body Systems* (Springer, New York, 1998).

[55] Yu. V. Sharvin, Zh. Eksp. Teor. Fiz **48**, 984 (1965), [Sov. Phys. JETP **21**, 655 (1965)].

[56] A. Marchenkov, R. W. Simmonds, J. C. Davis, and R. E. Packard, Phys. Rev. B **65**, 075414 (2002).

[57] S. Datta, *Electronic Transport in Mesoscopic Systems* (Cambridge University Press, Cambridge, 1995).

[58] S. N. Artemenko, A. F. Volkov, and A. V. Zaitsev, Zh. Eksp. Teor. Fiz. **76**, 1816 (1979), [Sov. Phys. JETP **49**, 924-931 (1979)].

[59] A. V. Zaitsev, Zh. Eksp. Teor. Fiz. **78**, 221 (1980), [Sov. Phys. JETP **51**, 111-116 (1980)], Erratum: Zh. Eksp. Teor. Fiz. **79**, 2016 (1980) [Sov. Phys. JETP **52**, 1018 (1980)].

[60] U. Gunsenheimer and A. Zaikin, Phys. Rev. B **50**, 6317 (1994).

[61] D. Averin and A. Bardas, Phys. Rev. Lett. **75**, 1831 (1995).

[62] D. Averin and A. Bardas, Phys. Rev. B **53**, R1705 (1996).

[63] D. Averin, cond-mat/9803065.

[64] M. Eschrig, Phys. Rev. B **61**, 9061 (2000).

[65] Yu. Mukharsky, J. Low Temp. Phys. **134**, 731 (2004).

[66] E. V. Thuneberg, Phys. Rev. B **36**, 3583 (1987).

[67] A. L. Fetter and S. Ullah, J. Low Temp. Phys. **70**, 515 (1988).

[68] A. J. Leggett and S.-K. Yip, in *Helium Three*, edited by W. P. Halperin and L. P. Pitaevskii (North-Holland, Amsterdam, 1990).

[69] D. D. Osheroff and M. C. Cross, Phys. Rev. Lett. **18**, 905 (1977).

[70] J. A. Sauls and J. W. Serene, Phys. Rev. B **24**, 183 (1981).

[71] N. Schopohl, Phys. Rev. Lett. **58**, 1664 (1987).

[72] A. J. Leggett and S. Takagi, Ann. Phys. **106**, 79 (1977).

Abstracts of publications

[P1] The flow of superfluid ^{3}He-B through a 65 x 65 array of nanometer-size apertures has been measured recently by Backhaus *et al.* They find in the current-phase relation a new branch, the so-called π state. We study two limiting cases which show that the pi state arises from the coupling of the phase degree of freedom to the spin-orbit rotation. The π state exists in a single large aperture, but is difficult to observe because of hysteresis. A better correspondence with experiments is obtained by assuming a thin wall, where the Josephson coupling between the two sides arises from a dense array of pinholes.

[P2] We theoretically study the dc Josephson effect between two volumes of superfluid ^{3}He-B. We first discuss how the calculation of the current-phase relationships is divided into mesoscopic and macroscopic problems. We then analyze mass and spin currents and the symmetry of weak links. In quantitative calculations the weak link is assumed to be a pinhole, whose size is small in comparison to the coherence length. We derive a quasiclassical expression for the coupling energy of a pinhole, also allowing for scattering in the hole. Using a self-consistent order parameter near a wall, we calculate the current-phase relationships in several cases. In the isotextural case, the current-phase relations are plotted assuming a constant spin-orbit texture. In the opposite anisotextural case the texture changes as a function of the phase difference. For this we have to consider the stiffness of the macroscopic texture, and we also calculate some surface interaction parameters. We analyze the experiments by Marchenkov *et al.*, [Phys. Rev. Lett. **83**, 3860 (1999)], although the assumptions of the pinhole model were not quite satisfied there. We find that the observed π states and bistability can hardly be explained with the isotextural pinhole model, but a quantitative agreement is achieved with the anisotextural model.

[P3] A two-dimensional Ginzburg-Landau theory of weak links in a p-wave superfluid is presented. First we consider the symmetry properties of the energy functionals, and their relation to the conserved supercurrents which play an essential role in the weak link problem. In numerical studies, we use the A and B phases of superfluid ^{3}He. The phases on the two sides of the weak link can be chosen separately, and very general soft degrees of freedom may be imposed as boundary conditions. We study all four inequivalent combinations of A and B which are possible for a hole in a planar wall, including weak links with a pinned A-B interface. In all cases, some illustrative current-phase relations

(CPR's) are calculated and the critical currents are mapped. Phase diagrams covering the relevant phase space in zero magnetic field are constructed. The numerical methods are also described in some detail.

[P4] We report on a Ginzburg-Landau calculation of the stability of a boundary between A and B phases of superfluid ^{3}He in a two-dimensional constriction. In the macroscopic limit the stability follows a well-known relation, which depends on the surface tension σ_{AB} of the A-B boundary. In the narrow-constriction limit the surface tension is not well defined, but the interface is always stable, and a weak link between the A and B phases is obtained.

[P5] Recent measurements of dissipative currents in pressure-biased weak links of superfluid ^{3}He-B are discussed. It is pointed out that the theoretical understanding of their results is unsatisfactory. As one candidate model to explain them, we consider the process of multiple Andreev reflections (MAR). Connection of MAR to bound quasiparticle states inside ballistic contacts is discussed. As an explicit example we analyze the current in a short pressure-biased ballistic ^{3}He-B constriction. It is shown that the dissipative part of the current does not depend on the spin-orbit rotation matrices.

[P6] We calculate the current-pressure relation for pinholes connecting two volumes of bulk superfluid ^{3}He-B. The theory of multiple Andreev reflections, adapted from superconducting weak links, leads to a nonlinear dependence of the dc current on pressure bias. In arrays of pinholes one has to take into account oscillations of the texture at the Josephson frequency. The associated radiation of spin waves from the junction leads to an additional dissipative current at small biases, in quantitative agreement with measurements.